

# Instrumentation and 5-Year Performance Monitoring of a GRS-IBS in St. Lawrence County, NY

PUBLICATION NO. FHWA-HRT-20-040

MAY 2020



U.S. Department of Transportation  
**Federal Highway Administration**

Research, Development, and Technology  
Turner-Fairbank Highway Research Center  
6300 Georgetown Pike  
McLean, VA 22101-2296

## FOREWORD

This report summarizes the instrumentation and monitoring program for a Geosynthetic Reinforced Soil–Integrated Bridge System (GRS-IBS) project constructed under FHWA’s Every Day Counts program. This instrumentation and monitoring were undertaken to better understand the substructure–superstructure interaction of the bridge. The GRS-IBS in St. Lawrence County, NY was chosen for long-term monitoring because its span length, skew, and superelevation were relatively unique at the time.

In addition to presenting the performance results of the instrumentation, this report highlights many of the basic steps necessary to successfully monitor bridge performance with a remote data-acquisition system (RDAS). Information about the instrumentation, testing requirements and logistics, installation procedures, RDAS setup, and general lessons learned from this GRS-IBS project is included.

This report will be useful to bridge designers interested in learning more about the performance and substructure–superstructure interaction of this type of bridge system and to practitioners and researchers using RDASs for geotechnical applications.

Cheryl Allen Richter, PhD, PE  
Director, Office of Infrastructure  
Research and Development

### Notice

This document is disseminated under the sponsorship of the U.S. Department of Transportation (USDOT) in the interest of information exchange. The U.S. Government assumes no liability for the use of the information contained in this document.

The U.S. Government does not endorse products or manufacturers. Trademarks or manufacturers’ names appear in this report only because they are considered essential to the objective of the document.

### Quality Assurance Statement

The Federal Highway Administration (FHWA) provides high-quality information to serve Government, industry, and the public in a manner that promotes public understanding. Standards and policies are used to ensure and maximize the quality, objectivity, utility, and integrity of its information. FHWA periodically reviews quality issues and adjusts its programs and processes to ensure continuous quality improvement.

## TECHNICAL REPORT DOCUMENTATION PAGE

1. Report No. FHWA-HRT-20-040	2. Government Accession No.	3. Recipient's Catalog No.	
4. Title and Subtitle Instrumentation and 5-Year Performance Monitoring of a GRS-IBS in St. Lawrence County, NY		5. Report Date May 2020	
		6. Performing Organization Code: HRDI-40	
7. Author(s) Jennifer Nicks (ORCID: 0000-0001-7230-3578), Michael Adams, Tom Stabile, and Jan Li		8. Performing Organization Report No.	
9. Performing Organization Name and Address Office of Infrastructure Research and Development Turner-Fairbank Highway Research Center 6300 Georgetown Pike McLean, VA 22101		10. Work Unit No.	
		11. Contract or Grant No. N/A	
12. Sponsoring Agency Name and Address Office of Infrastructure Research and Development Turner-Fairbank Highway Research Center 6300 Georgetown Pike McLean, VA 22101		13. Type of Report and Period Covered Technical Report; 2013–2018	
		14. Sponsoring Agency Code HRDI-40	
15. Supplementary Notes The Contracting Officer's Representative was Michael Adams. The lab support contractors (Tom Stabile and Jan Li) were under DTFH61-12-D-00008-T-13006.			
16. Abstract One of the first Geosynthetic Reinforced Soil–Integrated Bridge System (GRS-IBS) projects to be instrumented and evaluated under the Federal Highway Administration's (FHWA's) Every Day Counts program was a replacement bridge along County Road 47 over Trout Brook in the town of Stockholm within St. Lawrence County, NY. This GRS-IBS is aligned on a 30-degree skew with a 3.65-percent superelevation and a 0.5-percent grade. The new superstructure consists of 105-ft steel multigirders and prefabricated-concrete deck panels. The heights of the north and south geosynthetic–reinforced soil abutments were 11.0 and 11.6 ft, respectively. To evaluate the performance of this bridge, FHWA instrumented and monitored the bridge for over 5 years. This report details the results of the instrumentation installation and findings from this bridge evaluation. Overall, performance has been excellent, well within the expectations based on previous structures. Key results include measured vertical and lateral earth pressures, lateral deformations at the face and behind the backwall of the superstructure, and vertical and differential settlements.			
17. Key Words Geosynthetic reinforced soil, integrated bridge system, abutment, remote data-acquisition system, pressure cell, in-place inclinometer, performance monitoring, differential settlement, earth pressures, lateral deformation		18. Distribution Statement No restrictions. This document is available to the public through the National Technical Information Service, Springfield, VA 22161. <a href="http://www.ntis.gov">http://www.ntis.gov</a>	
19. Security Classif. (of this report) Unclassified	20. Security Classif. (of this page) Unclassified	21. No. of Pages 55	22. Price N/A

## SI\* (MODERN METRIC) CONVERSION FACTORS

### APPROXIMATE CONVERSIONS TO SI UNITS

Symbol	When You Know	Multiply By	To Find	Symbol
<b>LENGTH</b>				
in	inches	25.4	millimeters	mm
ft	feet	0.305	meters	m
yd	yards	0.914	meters	m
mi	miles	1.61	kilometers	km
<b>AREA</b>				
in <sup>2</sup>	square inches	645.2	square millimeters	mm <sup>2</sup>
ft <sup>2</sup>	square feet	0.093	square meters	m <sup>2</sup>
yd <sup>2</sup>	square yard	0.836	square meters	m <sup>2</sup>
ac	acres	0.405	hectares	ha
mi <sup>2</sup>	square miles	2.59	square kilometers	km <sup>2</sup>
<b>VOLUME</b>				
fl oz	fluid ounces	29.57	milliliters	mL
gal	gallons	3.785	liters	L
ft <sup>3</sup>	cubic feet	0.028	cubic meters	m <sup>3</sup>
yd <sup>3</sup>	cubic yards	0.765	cubic meters	m <sup>3</sup>
NOTE: volumes greater than 1,000 L shall be shown in m <sup>3</sup>				
<b>MASS</b>				
oz	ounces	28.35	grams	g
lb	pounds	0.454	kilograms	kg
T	short tons (2,000 lb)	0.907	megagrams (or "metric ton")	Mg (or "t")
<b>TEMPERATURE (exact degrees)</b>				
°F	Fahrenheit	5 (F-32)/9 or (F-32)/1.8	Celsius	°C
<b>ILLUMINATION</b>				
fc	foot-candles	10.76	lux	lx
fl	foot-Lamberts	3.426	candela/m <sup>2</sup>	cd/m <sup>2</sup>
<b>FORCE and PRESSURE or STRESS</b>				
lbf	poundforce	4.45	newtons	N
lbf/in <sup>2</sup>	poundforce per square inch	6.89	kilopascals	kPa
<b>APPROXIMATE CONVERSIONS FROM SI UNITS</b>				
Symbol	When You Know	Multiply By	To Find	Symbol
<b>LENGTH</b>				
mm	millimeters	0.039	inches	in
m	meters	3.28	feet	ft
m	meters	1.09	yards	yd
km	kilometers	0.621	miles	mi
<b>AREA</b>				
mm <sup>2</sup>	square millimeters	0.0016	square inches	in <sup>2</sup>
m <sup>2</sup>	square meters	10.764	square feet	ft <sup>2</sup>
m <sup>2</sup>	square meters	1.195	square yards	yd <sup>2</sup>
ha	hectares	2.47	acres	ac
km <sup>2</sup>	square kilometers	0.386	square miles	mi <sup>2</sup>
<b>VOLUME</b>				
mL	milliliters	0.034	fluid ounces	fl oz
L	liters	0.264	gallons	gal
m <sup>3</sup>	cubic meters	35.314	cubic feet	ft <sup>3</sup>
m <sup>3</sup>	cubic meters	1.307	cubic yards	yd <sup>3</sup>
<b>MASS</b>				
g	grams	0.035	ounces	oz
kg	kilograms	2.202	pounds	lb
Mg (or "t")	megagrams (or "metric ton")	1.103	short tons (2,000 lb)	T
<b>TEMPERATURE (exact degrees)</b>				
°C	Celsius	1.8C+32	Fahrenheit	°F
<b>ILLUMINATION</b>				
lx	lux	0.0929	foot-candles	fc
cd/m <sup>2</sup>	candela/m <sup>2</sup>	0.2919	foot-Lamberts	fl
<b>FORCE and PRESSURE or STRESS</b>				
N	newtons	2.225	poundforce	lbf
kPa	kilopascals	0.145	poundforce per square inch	lbf/in <sup>2</sup>

\*SI is the symbol for International System of Units. Appropriate rounding should be made to comply with Section 4 of ASTM E380. (Revised March 2003)

## TABLE OF CONTENTS

<b>CHAPTER 1. INTRODUCTION .....</b>	<b>1</b>
<b>Background .....</b>	<b>1</b>
<b>CR47 GRS-IBS—Abutment Details.....</b>	<b>2</b>
<b>Instrumentation Objectives.....</b>	<b>2</b>
<b>CHAPTER 2. INSTRUMENTATION PROGRAM.....</b>	<b>3</b>
<b>Background .....</b>	<b>3</b>
<b>Pre-Installation Testing and Logistics .....</b>	<b>5</b>
<b>Instrumentation Installation .....</b>	<b>6</b>
Vertical Pressure Cells .....	7
Contact Pressure Cells .....	10
IPIs .....	11
RDAS .....	18
Survey Targets .....	20
<b>Lessons Learned.....</b>	<b>22</b>
Data-Acquisition System .....	23
Cable Protection.....	23
RDAS Mounting .....	23
Data Collection Memory.....	23
Maintenance .....	23
Surveying .....	24
<b>CHAPTER 3. PERFORMANCE MONITORING.....</b>	<b>25</b>
<b>Vertical Earth Pressures .....</b>	<b>25</b>
During Construction.....	26
Post-Construction.....	28
<b>Lateral Earth Pressures .....</b>	<b>30</b>
During Construction.....	30
Post-Construction.....	31
Lateral Deformations .....	34
Vertical Settlement and Strain .....	39
<b>CHAPTER 4. SUMMARY AND CONCLUSIONS.....</b>	<b>45</b>
<b>REFERENCES.....</b>	<b>47</b>

## LIST OF FIGURES

Figure 1. Photo. CR47 GRS-IBS over Trout Brook. ....	1
Figure 2. Illustration. Design cross section for the CR47 GRS-IBS over Trout Brook. ....	2
Figure 3. Illustration. Cross section of instrumentation for the south abutment of the CR47 GRS-IBS. ....	3
Figure 4. Illustrations. Location and nomenclature of abutment instrumentation. ....	4
Figure 5. Location and nomenclature of IPIs. ....	5
Figure 6. Photo. VPCs on sand bedding. ....	8
Figure 7. Photo. VPC positioning and cable trench bedded with sand. ....	8
Figure 8. Photo. VPCs with sand cover. ....	9
Figure 9. Photo. Paint marks showing the locations of VPCs at the base of the south abutment’s footing formwork. ....	9
Figure 10. Photo. CPCs with grout bed mounted on the northwest cheek wall. ....	10
Figure 11. Photos. CPCs on the back and cheek walls. ....	10
Figure 12. Photos. Installation of CPCs with a plywood sheet as form for the sand layer. ....	11
Figure 13. Illustrations. Locations of IPI strings at the north and south abutments. ....	12
Figure 14. Photo. IPI casing installed and grouted in the south abutment foundation. ....	13
Figure 15. Photo. Aligning the IPI casing with the centerline of the bridge. ....	13
Figure 16. Photo. Geotextile threaded over the IPI casing. ....	14
Figure 17. Photo. Steel straps and a protective aggregate layer securing the IPI casing to the south abutment wall. ....	14
Figure 18. Photo. Steel-channel shield protecting the IPI casing on the south abutment wall. ....	15
Figure 19. Photos. IPI casings along the backwall on the north and south abutments. ....	15
Figure 20. Photo. IPIs and jumper cables. ....	16
Figure 21. Photo. IPI wheel assembly on the south abutment (fixed wheel is on the right, toward the abutment). ....	17
Figure 22. Photos. Hanging bracket on top of the IPI-S-Back casing and protective PVC sleep and cap. ....	17
Figure 23. Photo. Protective cap on the IPI-S-Face casing. ....	18
Figure 24. Photo. RDAS components. ....	19
Figure 25. Photo. RDAS components mounted to a wooden post installed near the wing wall. ....	19
Figure 26. Photo. Flexible conduit carrying north abutment instrumentation cables. ....	20
Figure 27. Photo. Total-station mounting post. ....	21
Figure 28. Illustration. Location of survey targets on the north abutment wall and beam footing. ....	21
Figure 29. Photo. Reflective survey target and swivel attached to GRS facing blocks. ....	22
Figure 30. Photo. Survey targets attached to footing formwork and a GRS facing block. ....	22
Figure 31. Charts. Vertical earth pressures during construction of the north and south abutments. ....	27
Figure 32. Charts. Vertical earth pressures under north and south abutment footings. ....	28
Figure 33. Chart. Comparison of average vertical earth pressures on the north and south abutments. ....	29

Figure 34. Charts. Lateral earth pressures during construction of the north and south abutments. ....	31
Figure 35. Chart. Lateral earth pressures and temperatures behind backwalls.....	32
Figure 36. Chart. Lateral earth pressures on cheek walls. ....	32
Figure 37. Chart. Relationship between vertical and lateral earth pressures for the north and south abutments. ....	33
Figure 38. Chart. Cumulative displacement for IPI-S-Back.....	34
Figure 39. Chart. Cumulative displacement for IPI-S-Face. ....	35
Figure 40. Chart. Cumulative displacement for IPI-N-Back. ....	35
Figure 41. Chart. Incremental displacement for IPI-S-Back. ....	37
Figure 42. Chart. Incremental displacement for IPI-S-Face. ....	37
Figure 43. Chart. Incremental displacement for IPI-N-Back.....	38
Figure 44. Chart. Relationship between maximum cumulative IPI displacement and lateral earth pressures behind the backwalls.....	39
Figure 45. Charts. Vertical settlement of the north and south abutments.....	40
Figure 46. Chart. Vertical strain of the abutments based on their height. ....	41
Figure 47. Charts. 100-year forecast for settlement and vertical strain of the north and south abutments. ....	42
Figure 48. Chart. Differential settlement between the north and south abutments.....	43

## LIST OF TABLES

Table 1. Construction activity and corresponding instrumentation.....	6
Table 2. Timeline of construction and instrumentation events.....	7
Table 3. Instrumentation nomenclature. ....	25

## LIST OF ABBREVIATIONS

CMU	concrete masonry unit
CPC	contact pressure cell
CR	County Road
DL	dead load
EDC-1	Every Day Counts initiative, round 1
FHWA	Federal Highway Administration
GP	Poorly graded gravel
GRS	geosynthetic reinforced soil
GRS-IBS	Geosynthetic Reinforced Soil–Integrated Bridge System
IPI	in-place inclinometer
IPI-N-Back	in-place inclinometer installed on the backwall of the north abutment
IPI-S-Back	in-place inclinometer installed on the backwall of the south abutment
IPI-S-Face	in-place inclinometer installed on the face of the south abutment
LP-N-Back	lateral pressure cell installed on the backwall of the north abutment
LP-N-East	lateral pressure cell installed on the east cheek wall of the north abutment
LP-N-West	lateral pressure cell installed on the west cheek wall of the north abutment
LP-S-Back	lateral pressure cell installed on the backwall of the south abutment
LP-S-East	lateral pressure cell installed on the east cheek wall of the south abutment
LP-S-West	lateral pressure cell installed on the west cheek wall of the south abutment
MEMS	micro-electro-mechanical systems
PVC	polyvinyl chloride
RDAS	remote data-acquisition system
RSF	reinforced soil foundation
TFHRC	Turner-Fairbank Highway Research Center
VP-N-AVG	average vertical pressure from VP-N-Back, VP-N-Face, and VP-N-Mid
VP-N-Back	vertical pressure cell installed furthest from the face of the north abutment
VP-N-Face	vertical pressure cell installed closest to the face of the north abutment
VP-N-Mid	vertical pressure cell installed under the middle of the footing on the north abutment
VP-S-AVG	average vertical pressure from VP-S-Back, VP-S-Face, and VP-S-Mid
VP-S-Back	vertical pressure cell installed furthest from the face of the south abutment
VP-S-Face	vertical pressure cell installed closest to the face of the south abutment
VP-S-Mid	vertical pressure cell installed under the middle of the footing on the south abutment
VPC	vertical pressure cell



## CHAPTER 1. INTRODUCTION

### BACKGROUND

In the first round of the Federal Highway Administration’s (FHWA’s) Every Day Counts initiative (EDC-1), FHWA promoted Geosynthetic Reinforced Soil–Integrated Bridge Systems (GRS-IBSs) for rapid deployment around the country because of the time and cost savings they have brought to projects. In addition, the performance of such systems was proven to be reliable for the bridge characteristics (e.g., span length, grade, skew, average daily traffic, etc.) that had been constructed at that time. As additional bridges were designed and constructed near or outside the initial maximum limits of those characteristics, FHWA set up an instrumentation and monitoring program to evaluate several bridges and determine whether changes in design guidelines were necessary as the bounds of GRS-IBS applications were extended.

One of the first GRS-IBS projects to be instrumented and evaluated in EDC-1 was a replacement bridge along County Road (CR) 47 over Trout Brook in the town of Stockholm within St. Lawrence County, NY, hereafter referred to as “the CR47 GRS-IBS.” This GRS-IBS is aligned on a 30-degree skew with a 3.65-percent superelevation (east-to-west downward slope) and a 0.5-percent grade. The south abutment is at a slightly higher elevation than the north abutment. The new superstructure consists of 105-ft steel multigirders and prefabricated concrete deck panels. The heights of the north and south geosynthetic–reinforced soil (GRS) abutments were 11.0 and 11.6 ft, respectively. Construction of this replacement bridge began in May 2013, and the bridge was opened to traffic in October 2013. The design and construction of the bridge was performed per interim FHWA guidelines (Adams et al. 2011). Current FHWA guidance, however, is provided by Adams and Nicks (2018). Figure 1 shows the completed bridge.

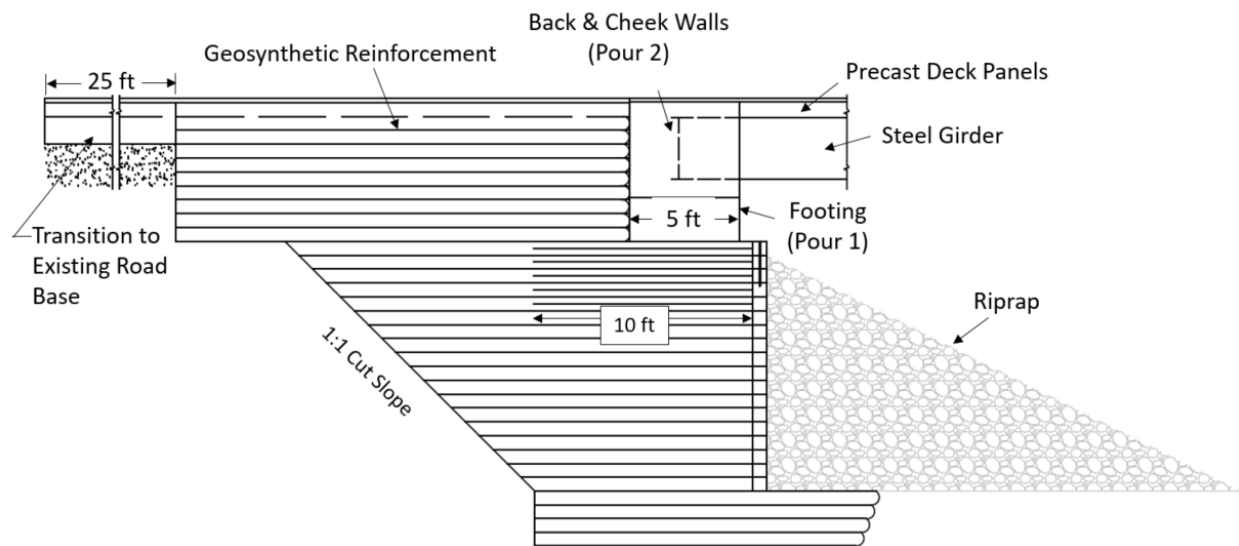


Source: FHWA.

**Figure 1. Photo. CR47 GRS-IBS over Trout Brook.**

## CR47 GRS-IBS—ABUTMENT DETAILS

The abutments of the CR47 GRS-IBS were constructed with a compacted, clean, crushed aggregate that had grain sizes ranging from 0.25 to 1 inch and was layered with a woven 4,800 lb/ft geotextile placed at a nominal 8-inch spacing. The aggregate was classified as a poorly graded gravel (GP), an A-1-a, or a No. 1 according to the Unified Soil Classification System, the American Association of State Highway Transportation Officials Classification System, and the New York State Department of Transportation, respectively (ASTM D2487 2017; AASHTO 2017; NYSDOT 2014). The assumed unit weight and friction angle of the structural backfill for the design were 110 lb/ft<sup>3</sup> and 40 degrees. The facing blocks consist of 7<sup>5</sup>/<sub>8</sub>- by 7<sup>5</sup>/<sub>8</sub>- by 15<sup>5</sup>/<sub>8</sub>-inch solid concrete masonry units (CMUs). The geotextile reinforcement extended through each dry-stacked course of block, creating a frictional connection with the CMUs. The abutments were founded on a reinforced soil foundations (RSFs) underlain by a dense glacial till. Figure 2 is a cross section of the layout of the south abutment.



Source: FHWA.

**Figure 2. Illustration. Design cross section for the CR47 GRS-IBS over Trout Brook.**

## INSTRUMENTATION OBJECTIVES

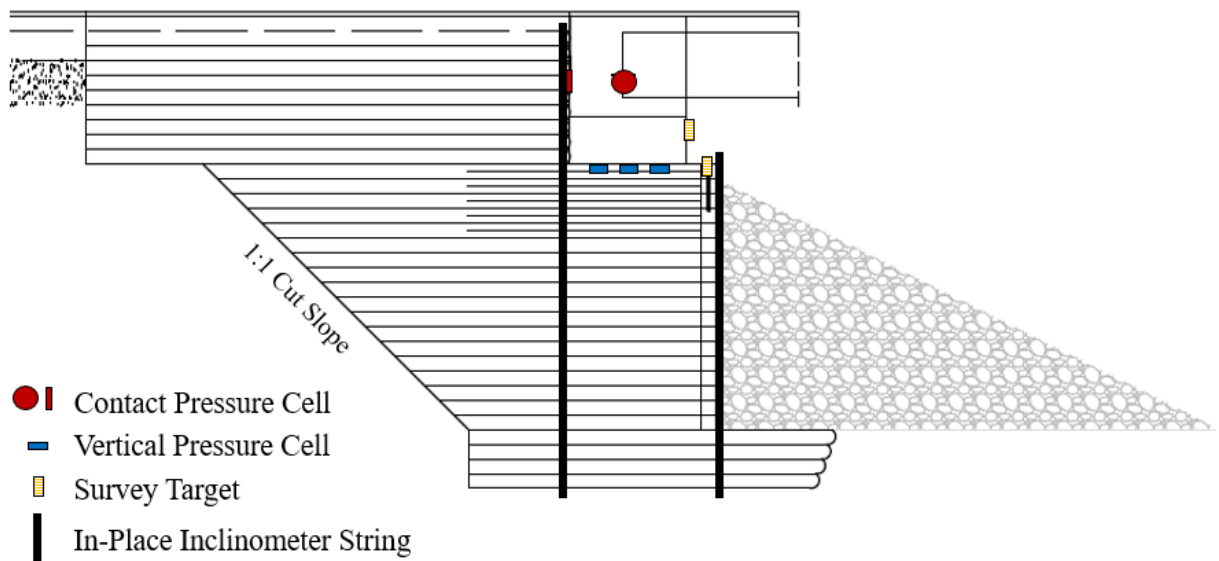
To monitor the performance of the CR47 GRS-IBS, FHWA developed an instrumentation program. The objectives were to evaluate deformations and investigate substructure–superstructure interaction. The impacts of skew, grade, and span length on performance can also be analyzed by comparing these characteristics across other GRS-IBSs that have been monitored.

This report outlines the details of the instrumentation program, installation procedures, and setup of the remote data-acquisition system (RDAS) used to collect and transmit site data to FHWA’s Turner-Fairbank Highway Research Center (TFHRC). An evaluation of the CR47 GRS-IBS’s performance after 5 years in service is also presented. To date, no performance or maintenance issues with the bridge have been reported by the County.

## CHAPTER 2. INSTRUMENTATION PROGRAM

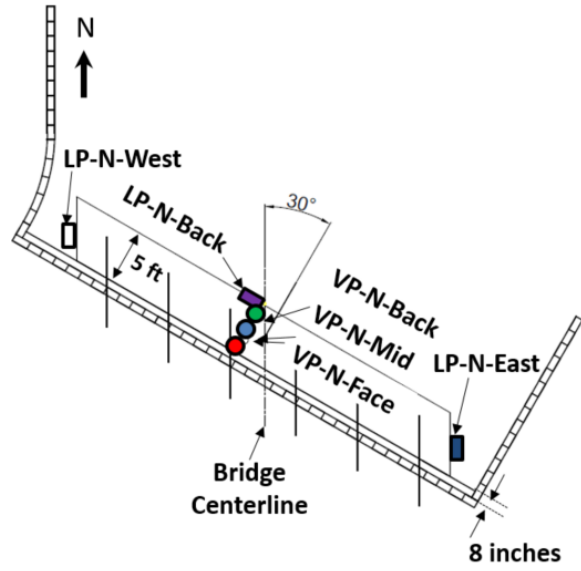
### BACKGROUND

FHWA designed the instrumentation program based on the factors of interest (e.g., skew, superelevation, and span length) and the budget available. Layouts of the sensors installed on the CR47 GRS-IBS are shown in figure 3 through figure 5; note that the north abutment of the bridge only had one in-place inclinometer (IPI) installed behind the backwall. To evaluate the impact of skew, the contact pressure between the reinforced backfill and the cheek walls of the superstructure backwall was monitored. Considering the span length of the bridge and the weather in St. Lawrence County, NY, the contact pressure and lateral deformation between the reinforced backfill and the backwall were monitored for thermal interaction. Finally, the vertical pressure was monitored at the front, middle, and back of the footing to evaluate the grade of the bridge. IPIs and survey targets on the face of the abutments were installed to measure lateral and vertical deformations over time.



Source: FHWA.

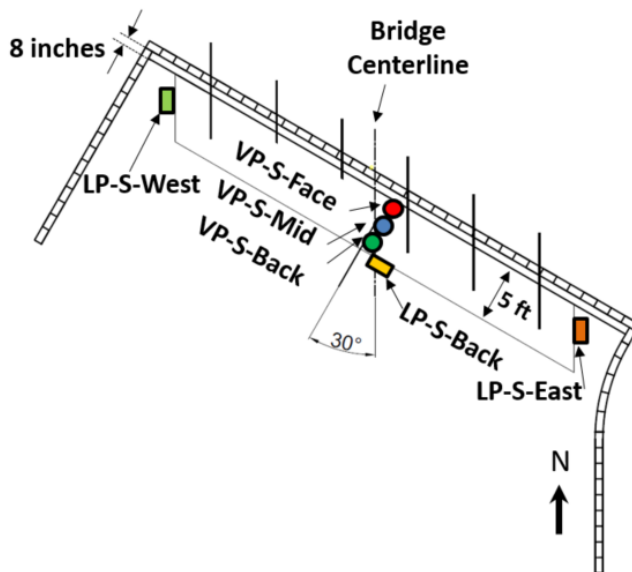
**Figure 3. Illustration. Cross section of instrumentation for the south abutment of the CR47 GRS-IBS.**



Source: FHWA.

N = north; LP-N-West = lateral pressure cell installed on the west cheek wall of the north abutment; LP-N-Back = lateral pressure cell installed on the backwall of the north abutment; VP-N-Back = vertical pressure cell installed furthest from the face of the north abutment; VP-N-Mid = vertical pressure cell installed under the middle of the footing on the north abutment; VP-N-Face = vertical pressure cell installed closest to the face of the north abutment; VP-N-East = vertical pressure cell installed on the east cheek wall of the north abutment.

A. North abutment.

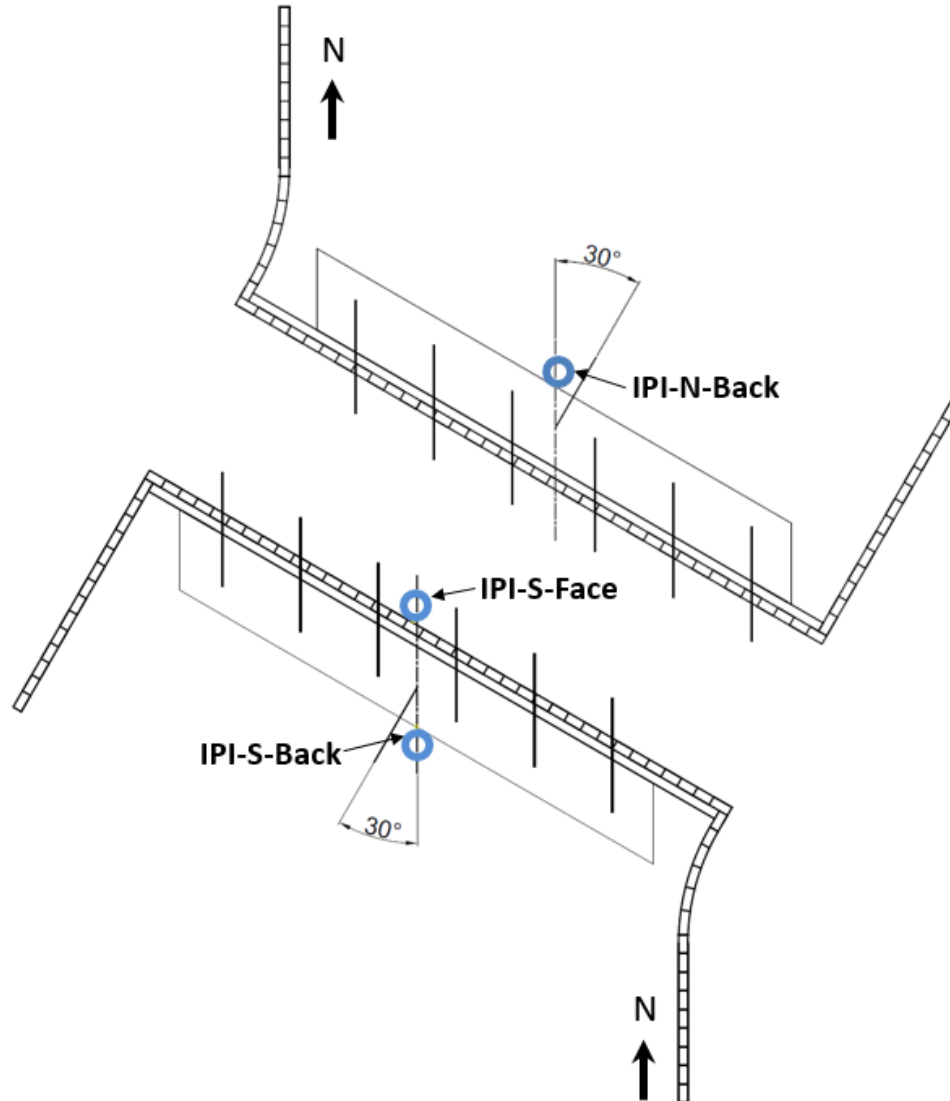


Source: FHWA.

N = north; LP-S-West = lateral pressure cell installed on the west cheek wall of the south abutment; VP-S-Face = vertical pressure cell installed closest to the face of the south abutment; VP-S-Mid = vertical pressure cell installed furthest from the face of the south abutment; VP-S-Back = vertical pressure cell installed furthest from the face of the south abutment; LP-S-Back = lateral pressure cell installed on the backwall of the south abutment; LP-S-East = lateral pressure cell installed on the east cheek wall of the south abutment.

B. South abutment.

**Figure 4. Illustrations. Location and nomenclature of abutment instrumentation.**



Source: FHWA.

N = north; IPI-N-Back = IPI installed on the backwall of the north abutment; IPI-S-Face = IPI installed on the face of the south abutment; IPI-S-Back = IPI installed on the backwall of the south abutment.

**Figure 5. Location and nomenclature of IPIs.**

## PRE-INSTALLATION TESTING AND LOGISTICS

All instrumentation, which was calibrated by the vendors, along with the RDAS were tested in the TFHRC geotechnical laboratory to ensure they were functioning properly prior to being sent to the project site for installation. The pressure cell outputs were verified by placing each cell into a load frame and incrementally loading it to a given pressure within the range of the cell. Weight was applied (in increments of 20-percent of the design capacity of the pressure cell) and held for 1 min up to 100 percent cell capacity. Pressures calculated using the cell manufacturer-supplied pressure equation and calibration factors matched the applied pressure measured from the loading device. The outputs from the probes in the IPIs were verified as well. Each probe was hung vertically and moved through a range of angles; the response was recorded by the RDAS data logger and was shown to measure the physical angle of the probe.

After operation was verified, all instrumentation was connected to the RDAS to verify whether the data logger program functioned properly and could transmit data collected from all the sensors via the cellular modem. As part of this system check, the entire system was run for a few days and monitored to ensure the sensor output was stable.

Because the cables for each type of sensor are installed by the manufacturer, the cable lengths must be known prior to procuring the instrumentation. For this project, initial cable lengths were determined by reviewing photos and scaling off plan drawings of the sites. Additional lengths of approximately 15 percent were added to the cable quantities to accommodate any field changes, obstructions, or repositioning of the RDAS.

## **INSTRUMENTATION INSTALLATION**

TFHRC staff made two trips to the CR47 GRS-IBS site to install the instrumentation during different stages of construction. Both trips were necessary to capture pertinent loading events, such as the casting of the beam footings and placement of the steel girders. Due to the numerous phases of construction that corresponded to instrumentation installation, additional installation assistance was required directly from the County.

Frequent communication with the project engineer and site supervisor was necessary during the preconstruction phase to ensure the instrumentation components were procured, tested, and available onsite for the initial installation, which was immediately after the foundation excavation. Table 1 shows the construction activities in relation to instrumentation that needed to be installed at that phase. Important milestones within the construction timelines are shown in table 2 along with the estimated vertical pressure added at key loading increments; this information is helpful in evaluating the instrumentation data and verifying trends within the results. Note that the dead load (DL) for each aspect was estimated based on the construction drawings and engineer’s estimate. The total applied DL pressure for the bridge is approximately 19 psi.

**Table 1. Construction activity and corresponding instrumentation.**

<b>Construction Activity</b>	<b>Instrumentation Installation</b>
South abutment foundation cut	Installed the bottom IPI casing in the foundation subgrade
North abutment foundation cut	Installed the bottom IPI casing in the foundation subgrade
South abutment wall construction	Attached the IPI casing to the face of the abutment wall and installed the IPI casing in the GRS abutment fill
North abutment wall construction	Installed the IPI casing in the GRS abutment fill
Form work for the footings on both abutments	Installed VPCs in the top GRS abutment layer, installed survey targets on GRS abutment wall face, and set up the RDAS to begin data collection
Forms from the footings on both abutments stripped	Installed survey targets on the footings (prior to setting the steel girders) and installed the wall face IPIs
Forms from both abutment backwalls stripped	Installed the CPCs and IPIs
Integrated approach construction	Finalized the location of the RDAS mounting post

VPC = vertical pressure cell; CPC = contact pressure cell.

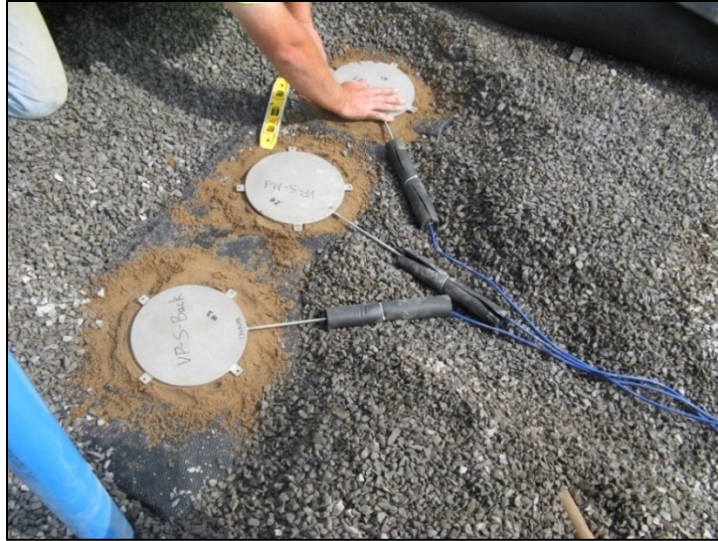
**Table 2. Timeline of construction and instrumentation events.**

<b>Key Construction/Instrumentation Events</b>	<b>Date</b>	<b>Applied DL Pressure (psi)</b>
Installed IPI-S-Face	7/1/2013	N/A
Installed VP-S-Face, VP-S-Mid, and VP-S-Back	7/1/2013	N/A
Installed VP-N-Face, VP-N-Mid, and VP-N-Back	7/2/2013	N/A
Cast concrete footings on both abutments (pour 1)	7/3/2013	2.1
Placed the steel girders	7/16/2013	9.1
Placed four (of eight) concrete deck panels	7/17/2013	
Placed remaining four concrete deck panels	7/18/2013	
Grouted deck joints w/UHPC	7/30/2013	
Cast the concrete back and cheek walls on both abutments (pour 2)	8/8/2013	4.7
Installed LP-N-Face, LP-N-East, and LP-N-West	8/12/2013	N/A
Installed LP-S-Face, LP-S-East, and LP-S-West	8/13/2013	N/A
Installed IPI-N-Back and IPI-S-Back	8/15/2013	N/A
Paved asphalt concrete on approach roadway	9/5/2013	N/A
Paved the asphalt concrete on the bridge deck	9/9/2013	3.1
Opened bridge to traffic	10/10/2013	N/A

N/A = not applicable; VP-S-Face = vertical pressure cell installed closest to the face of the south abutment; VP-S-Mid = vertical pressure cell installed under the middle of the footing on the south abutment; VP-S-Back = vertical pressure cell installed furthest from the face of the south abutment; VP-N-Face = vertical pressure cell installed closest to the face of the north abutment; VP-N-Mid = vertical pressure cell installed under the middle of the footing on the north abutment; VP-N-Back = vertical pressure cell installed furthest from the face of the north abutment; LP-N-East = lateral pressure cell installed on the east cheek wall of the north abutment; LP-N-West = lateral pressure cell installed on the west cheek wall of the north abutment; LP-S-East = lateral pressure cell installed on the east cheek wall of the south abutment; LP-S-West = lateral pressure cell installed on the west cheek wall of the south abutment; IPI-S-Face = IPI installed on the face of the south abutment; IPI-N-Back = IPI installed on the backwall of the north abutment; IPI-S-Back = IPI installed on the backwall of the south abutment.

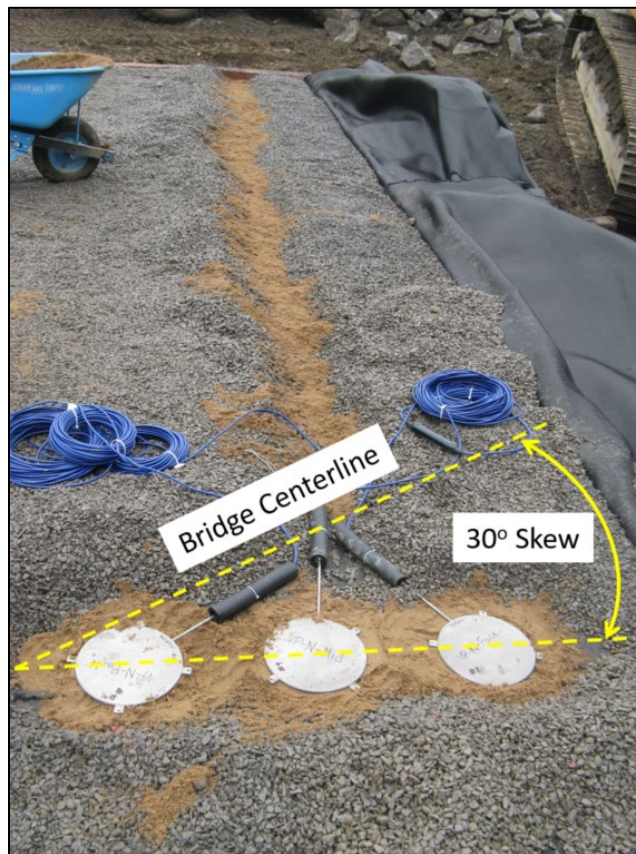
### **Vertical Pressure Cells**

Prior to constructing the formwork for the beam footing at each abutment, three vibrating-wire vertical pressure cells (VPCs) (with 9-inch diameters and capacities of 50 psi) were installed on the top layer of the GRS abutment, immediately beneath the concrete footing (figure 3). The VPCs measured the vertical stress at the top of the GRS abutment due to the weight of the superstructure. Figure 6 illustrates the installation of the VPCs prior to casting the concrete footing. The VPCs were positioned perpendicular to the abutment wall faces at an offset angle, equal to the skew, from the centerline of the bridge (figure 7) and layered in a sand bedding to provide an even contact area and eliminate the possibility of point loading from the crushed, aggregate fill (figure 8). The cables for the VPCs were embedded in a sand-filled trench (figure 7), which helped protect the cable from potential damage from compaction equipment during approach construction. The VPCs were then covered with a sheet of geotextile and their locations marked to help prevent damage during footing construction (figure 9). Pressure data were collected during the construction of the footing, which was cast in multiple stages.



Source: FHWA.

**Figure 6. Photo. VPCs on sand bedding.**



Source: FHWA.

**Figure 7. Photo. VPC positioning and cable trench bedded with sand.**



Source: FHWA.

**Figure 8. Photo. VPCs with sand cover.**



Source: FHWA.

**Figure 9. Photo. Paint marks showing the locations of VPCs at the base of the south abutment's footing formwork.**

## Contact Pressure Cells

Three contact pressure cells (CPCs) (with 9-inch diameters and capacities of 25 psi) were installed on each abutment to measure lateral earth pressures behind the backwall and on the cheek walls. For consistent pressure measurements, the position of each CPC was kept the same distance (44.5 inches) below the top of the bridge deck to the center of the CPC. Once the forms for the backwall and cheek walls were stripped, each CPC was attached by fastening four mounting tabs with plastic masonry anchors and screws. Prior to attaching the CPCs, a layer of cement grout was applied to each wall to provide a flat bearing area for the CPC (figure 10). It should be noted that the CPC mounted on the northwest cheek wall on the north abutment was damaged and is no longer operating. This cell may have been damaged during installation of the guide-rail post. Figure 11 shows the general locations of the CPCs attached to each abutment backwall and cheek wall.



Source: FHWA.

**Figure 10. Photo. CPCs with grout bed mounted on the northwest cheek wall.**



Source: FHWA.

A. CPC on the backwall.



Source: FHWA.

B. CPC on the cheek wall.

**Figure 11. Photos. CPCs on the back and cheek walls.**

Once the CPCs were attached, it was necessary to protect them from fill placement and compaction during approach construction. A protective sand layer was placed in front of each cell using a plywood sheet as a form (figure 12-A); the sheet was removed once fill material was placed (figure 12-B).



Source: FHWA.

A. Plywood sheet protection.



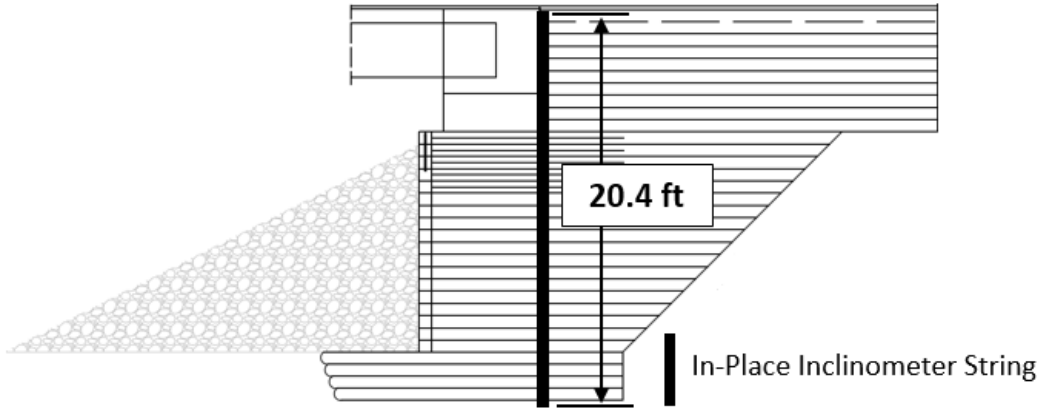
Source: FHWA.

B. Sand layer protection.

**Figure 12. Photos. Installation of CPCs with a plywood sheet as form for the sand layer.**

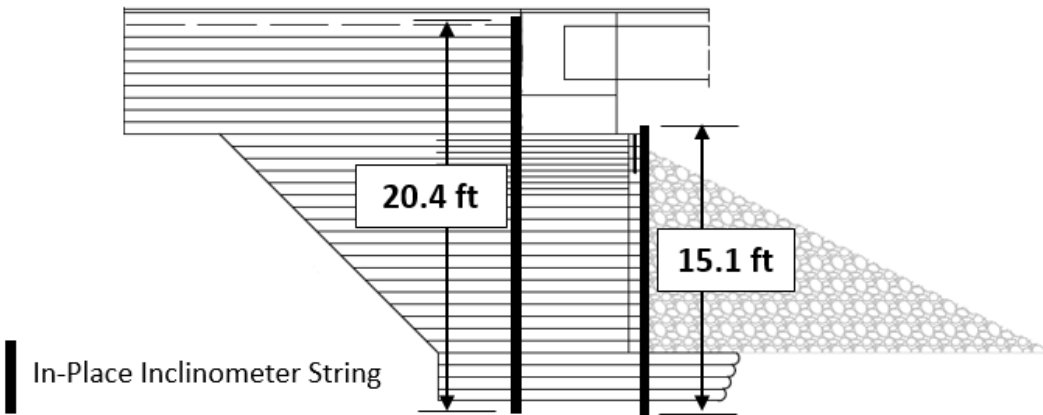
## IPIs

IPIs using micro-electro-mechanical systems (MEMS) were installed to monitor the lateral movement at the GRS fill–footing interface on each abutment (figure 13). The south abutment had an additional IPI attached to the CMU face to measure lateral deformation in that location. There were seven sensors located at depths of 2, 5.28, 8.56, 11.84, 15.12, 18.4, and 20.35 ft for the IPIs located behind the backwall on the north and south abutments. For the IPIs at the face of the south abutment, there were five sensors at depths of 0.2, 3.48, 6.76, 10.04, and 13.32 ft from the top of the abutment wall face. The casing that housed the IPIs was installed as the abutment was constructed.



Source: FHWA.

A. North abutment.



Source: FHWA.

B. South abutment.

**Figure 13. Illustrations. Locations of IPI strings at the north and south abutments.**

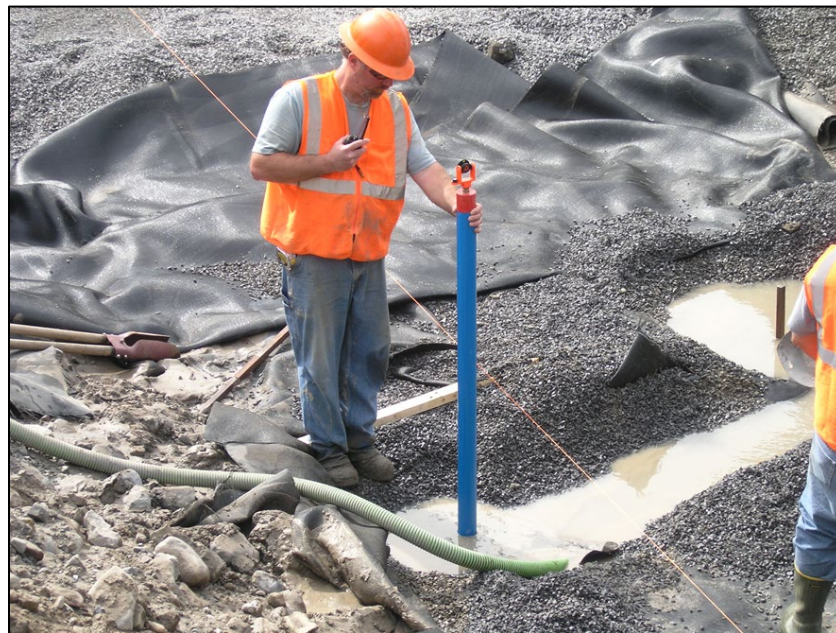
The County construction crew working on the bridge installed 5-ft sections of the IPI casing. The first section was anchored and grouted 2 ft below the foundation elevation in dense glacial till (figure 14). Before installation, a bottom cap was connected to the first casing section to keep the inside free of debris. For ease of assembly, 2.75-inch-outer-diameter quick-connect inclinometer casing was used. This type of casing has built-in couplings that snap together with no need for solvent cement or tape.



Source: FHWA.

**Figure 14. Photo. IPI casing installed and grouted in the south abutment foundation.**

Since the bridge was skewed, the grooves of the IPI casing were aligned perpendicularly to the superstructure and along the centerline to capture the movement of the bridge. A survey prism was placed on the casing section along with a transit for aligning the casing with the centerline (figure 15). The County crew continued installing the IPI casing in 5-ft sections during the construction of the abutments. The geotextile was slit and threaded over the casing (figure 16). Using this method of installation, the backfill surrounding the casing could be well compacted.



Source: FHWA.

**Figure 15. Photo. Aligning the IPI casing with the centerline of the bridge.**



Source: FHWA.

**Figure 16. Photo. Geotextile threaded over the IPI casing.**

The final sections of the IPI casing were added upon completion of the GRS wall. The casing for the IPI used to monitor the face of the south abutment was secured to the wall with pipe straps to keep it aligned vertically during construction (figure 17). The IPI casing was protected from damage during the placement of the riprap against the abutment wall face. The casing was surrounded by a layer of aggregate during the fill placement, and a section of steel channel was used to shield the casing in the zone of channel protection (figure 18).



Source: FHWA.

**Figure 17. Photo. Steel straps and a protective aggregate layer securing the IPI casing to the south abutment wall.**



Source: FHWA.

**Figure 18. Photo. Steel-channel shield protecting the IPI casing on the south abutment wall.**

On the north abutment, the position of the IPI casing within the GRS fill (IPI-N-Back) intersected the plane of the backwall, making it necessary for the casing to be partially cast into the backwall (figure 19-A). The IPI casing along the south abutment's backwall (IPI-S-Back) was about 2 inches away from the final line of the backwall. To keep the casing in contact with the wall and not cause any uneven bending during the approach fill placement, polyvinyl chloride (PVC) spacers were placed along the length of the casing and the casing was secured with pipe straps (figure 19-B).



Source: FHWA.

A. Embedded IPI-N-Back casing.



Source: FHWA.

B. IPI-S-Back casing with PVC spacers.

**Figure 19. Photos. IPI casings along the backwall on the north and south abutments.**

For continuous monitoring, MEMS IPI uniaxial sensors were installed to capture deformation along the length of the casing. IPIs were connected in series with jumper cables between each sensor instead of using one signal cable for each sensor (figure 20). This connection allowed for having only one cable connected to the RDAS data logger for each string of sensors.

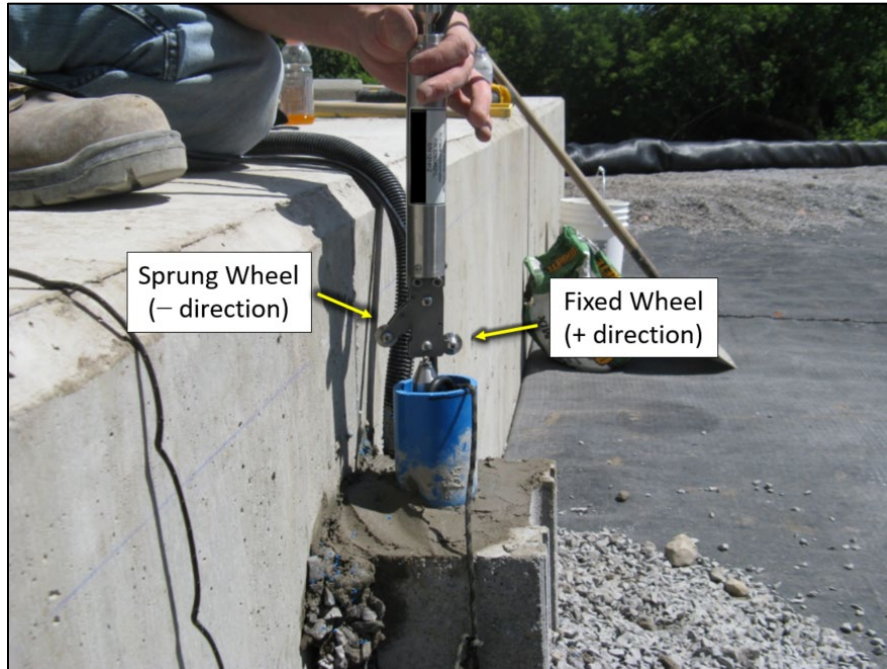


Source: FHWA.

**Figure 20. Photo. IPIs and jumper cables.**

The first step of installing the IPI string was to check the depth of the casing using a cloth measuring tape with a weighted end. Since the bottom sensor cannot touch the bottom of the casing, and the top elevation of the casing is fixed, any adjustments to the total string length could be made by shortening the gauge tube (i.e., the connecting rod attached to each sensor). Due to the short length of the sensor string, all the sensors and jumper cables were connected prior to being inserted into the casing. Electrical tape was used to hold the jumper cables and electrical connectors tightly against the gauge tubes. Securing the cables with tape helped prevent them from touching the walls of the casing. A nylon safety cord was attached to the bottom wheel assembly, allowing removal of the IPI string if necessary in the future. Once the IPI-array string was assembled, it was lowered into the casing, using care not to flex and strain the connection points of the gauge tubes.

The wheel assembly is part of the IPI. It contains a fixed and sprung wheel. The fixed wheel points in the direction of movement defined as the positive direction; in this case, the fixed wheel was pointed away from the stream channel for each string of IPIs (figure 21). After placement, a hanging bracket that allowed the string to be hung on the casing was connected to the top sensor, keeping the bottom sensor from contacting the casing bottom (figure 22).



Source: FHWA.

**Figure 21. Photo. IPI wheel assembly on the south abutment (fixed wheel is on the right, toward the abutment).**



Source: FHWA.

A. Hanging bracket.



Source: FHWA.

B. Protective sleeve.

**Figure 22. Photos. Hanging bracket on top of the IPI-S-Back casing and protective PVC sleep and cap.**

With each IPI string in place, a protective 4-inch PVC sleeve and cap was attached to the top of the casing. A slot was also cut into the PVC sleeve for the data cable to exit on the south abutment backwall. The sleeve was used to keep fill material from entering the casing and protect the top of the IPI string during the completion of construction. The IPI casing was embedded in the back of the north abutment, so for this set up, only the PVC cap was necessary. Similarly, only the protective cap was placed on the south abutment wall face's IPI (IPI-S-Face) because it was covered with steel pipe (figure 23).



Source: FHWA.

**Figure 23. Photo. Protective cap on the IPI-S-Face casing.**

## **RDAS**

A RDAS capable of remotely collecting and transmitting data from instrumentation during and after construction of the integrated bridge system was developed at TFHRC. Installation and setup of the RDAS occurred during the first trip to the site to begin recording initial readings of the VPCs prior to loading caused by casting of the footing. The system was then ready to capture the response to the weight of the beam footing, girders, precast deck panels, and asphalt wearing course. The data logger collection was initially set to a sample frequency of 1 reading per hour; however, to reduce the file size after a couple of years of monitoring, data from the VPCs, CPCs, and IPIs were collected only twice per day. The data were retrieved via a cellular modem and through an interfacing software package. The data files were then downloaded as text files and imported into a spreadsheet to perform analyses.

The RDAS base station was located on the south abutment side. The main components of the RDAS include the data logger, multiplexer, and cellular modem, all housed in a weather-proof box (figure 24). A deep-cycle marine battery housed in a separate metal battery box connected to a 50-watt solar panel was used to charge the battery. A cellular modem used an external antenna to connect and transmit data. The entire system was attached to a 4- by 4-inch post adjacent to the abutment (figure 25).



Source: FHWA.

**Figure 24. Photo. RDAS components.**



Source: FHWA.

**Figure 25. Photo. RDAS components mounted to a wooden post installed near the wing wall.**

All instrumentation on the north abutment (i.e., pressure cells and IPIs) was directly connected to the RDAS by cables that were placed in a flexible conduit, routed under the bridge, and secured by zip ties to sections of rebar that were tack welded to the girder. Figure 26 shows the conduit under the bridge containing signal cables from the north abutment pressure cells and IPI. It was important to have extra cable lengths available for the instrumentation sensors; this flexibility allowed for repositioning of the RDAS wooden post during construction and accommodated the increase in grade of the wing walls.



Source: FHWA.

**Figure 26. Photo. Flexible conduit carrying north abutment instrumentation cables.**

### **Survey Targets**

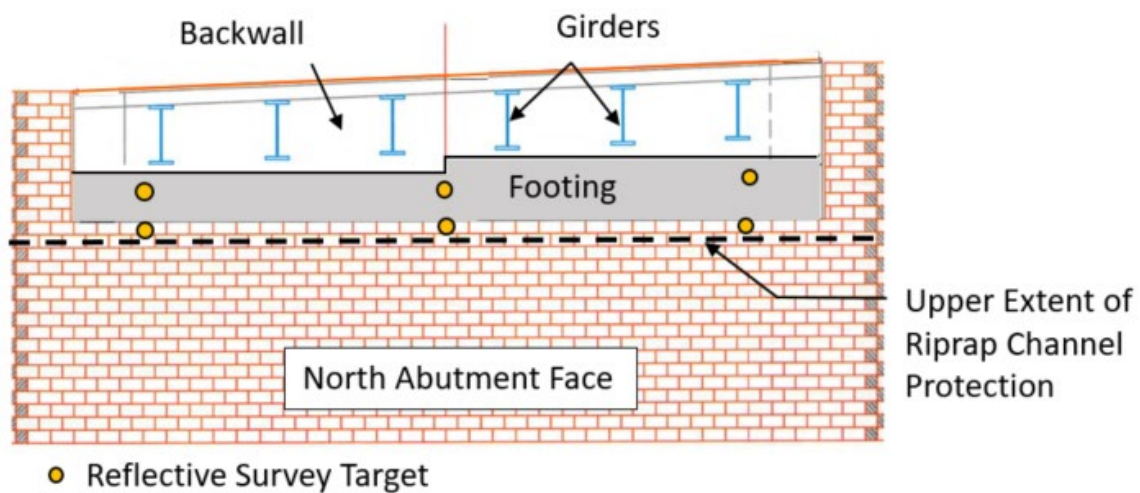
The survey-monitoring program consists of reflective targets and permanent total-station mounting posts. The total-station mounting posts were installed as the reference point for collecting all survey data (figure 27). The tops of the survey posts have threaded base plates that fit directly to the total station. The posts were set in concrete about 5 ft deep, beneath the assumed frost depth, and located in stable ground outside the potential flood zone.



Source: FHWA.

**Figure 27. Photo. Total-station mounting post.**

The total station has a 2 degree-angle and  $\pm 0.079$  inch-distance accuracy. The reflective survey targets were mounted on the abutment wall faces and footings to measure both wall and beam settlement. Three targets were attached to the GRS wall and three to the footing (figure 28). Survey targets on the lower portion of wall were not included because the wall was protected with riprap. The targets were mounted on an aluminum swivel arm, which allowed them to be aimed normal to the total station (figure 29). The aluminum swivel arm was fastened to the CMU block and concrete footing using plastic masonry anchors and construction adhesive. To capture the initial settlement during the casting of the beam footings, temporary targets were placed on the wooden formwork, and base line survey shots were collected (figure 30). These were later removed and attached permanently to the concrete footing.



Source: FHWA.

**Figure 28. Illustration. Location of survey targets on the north abutment wall and beam footing.**



Source: FHWA.

**Figure 29. Photo. Reflective survey target and swivel attached to GRS facing blocks.**



Source: FHWA.

**Figure 30. Photo. Survey targets attached to footing formwork and a GRS facing block.**

## **LESSONS LEARNED**

The St. Lawrence County instrumentation and monitoring program has been a valuable source of performance data for this GRS-IBS. Through hands-on experience preparing and installing the instrumentation along with reviewing the results, many lessons in developing a field-monitoring program were learned.

## **Data-Acquisition System**

Although components of a data-acquisition system are likely compatible with different types of instrumentation, it is better to choose devices and instrumentation from the same manufacturer to avoid uncertainty, especially for remote systems. In this study, for instance, the pressure cells and IPIs were based on different technologies and made by different manufacturers. If the original plan of the RDAS were applied, it would have not only increased the cost of the RDAS, but also caused difficulty assembling and programming the RDAS given the limited time available in the construction schedule. Fortunately, the limited distance between the two abutments allowed cables from the northern IPIs and pressure cells to be wired across the bridge and directly connected to the data acquisition–system base station located on the south abutment.

## **Cable Protection**

If cable protection from future construction activities that occur when the instrumentation-installation staff is offsite is needed, this concern must be communicated to the contractor (site superintendent). Surface markers are not always effective since the final grades are not constructed yet and markers can get filled over. As-built photos or drawings of the sensor locations presented to the contractor may help. In addition, sensor cables are often routed under or around form work and through site access paths. They should be marked while in temporary positions and placed inside a conduit to protect them from construction damage.

## **RDAS Mounting**

Drawings for the temporary locations of the mounting posts that will support the RDAS weather boxes, battery boxes, antenna, and solar panels should be provided. Their locations need to be flexible and movable during the construction of abutment layers. Extra cable lengths should be ordered to accommodate relocation. It is better to have too much cable, which can be spooled, than to have to make a field splice to add cable to reach the new position of the RDAS.

## **Data Collection Memory**

Based on the frequency of the readings from the connected instruments, the required memory capacity of the data logger should be predetermined. Site data should be downloaded before the data logger reaches full capacity since, at this point, the first record of data will be overwritten. In this project, a 4 MB external flash memory card was added to the data logger; with fewer than 30 sensors recording at 60-min intervals, the data could be downloaded from the data logger every month and never reach the limit of the data logger memory.

## **Maintenance**

Even though remote operation and data collection were set up for the instrumentation program, some site visits and maintenance should be expected. Since the instrumentation is contained in boreholes, the most likely maintenance activity would be repairing damaged cables. For the RDAS, typical maintenance activities include replacing dead batteries and cleaning solar panels. Other maintenance visits may be required due to malfunctioning RDAS components, vandalism, or storm damage.

## **Surveying**

Long-term survey monitoring at high degrees of accuracy in remote locations comes with challenges due to the potential lack of permanent survey control. The total station used to collect survey data for long-term monitoring possessed sufficient accuracy to measure small changes in deformation; however, the stability of the foundation for the total-station post over time may dictate the degree of accuracy from the measurements. With time, the ground surrounding the foundation of the total-station post can shrink and swell due to variations in seasonal temperature and precipitation. Additional benchmarks that limit relative movement would help reduce seasonal measurement changes.

### CHAPTER 3. PERFORMANCE MONITORING

After completing the instrumentation installation, the long-term performance of the north and south abutments along CR47 was monitored. The locations and nomenclature are described in table 3, figure 4, and figure 5. The nomenclature is used throughout the presentation of the results.

**Table 3. Instrumentation nomenclature.**

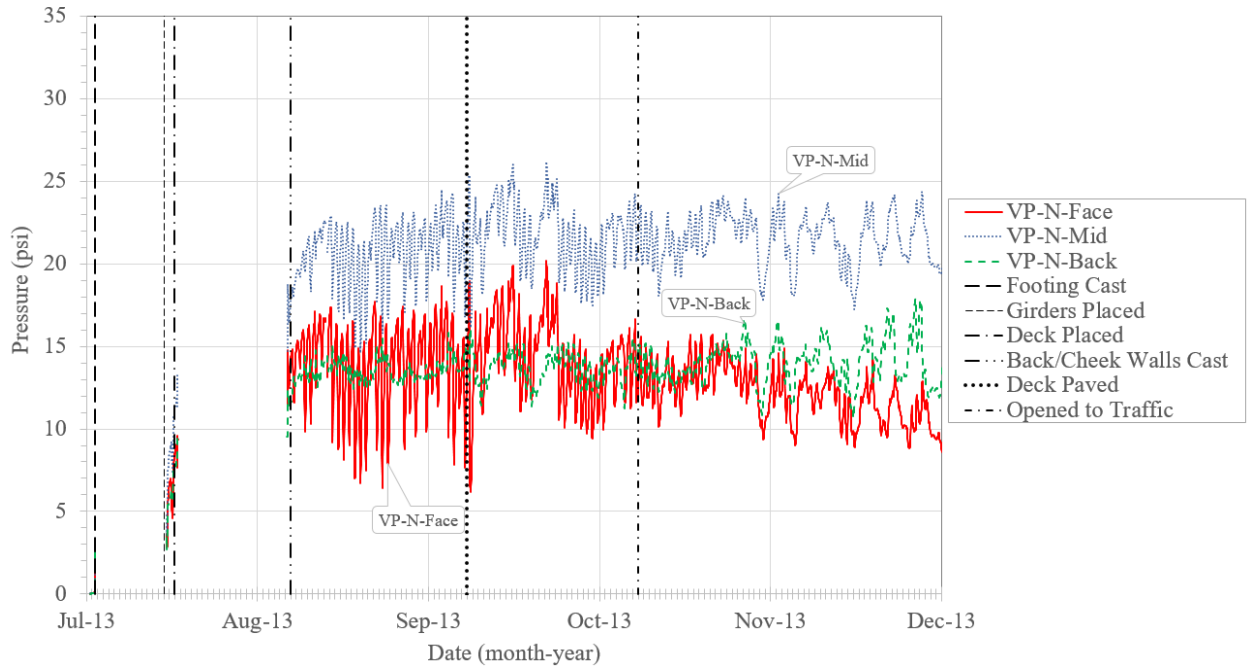
<b>Instrument</b>	<b>Abutment</b>	<b>Installation Location (see figure 4)</b>	<b>Nomenclature</b>	<b>Definition</b>
Vertical pressure cell	North	Face	VP-N-Face	Vertical pressure cell installed closest to the face of the north abutment
		Mid	VP-N-Mid	Vertical pressure cell installed under the middle of the footing on the north abutment
		Back	VP-N-Back	Vertical pressure cell installed furthest from the face of the north abutment
	South	Face	VP-S-Face	Vertical pressure cell installed closest to the face of the south abutment
		Mid	VP-S-Mid	Vertical pressure cell installed under the middle of the footing on the south abutment
		Back	VP-S-Back	Vertical pressure cell installed furthest from the face of the south abutment
Contact pressure cell	North	Back	LP-N-Back	Lateral pressure cell installed on the backwall of the north abutment
		East	LP-N-East	Lateral pressure cell installed on the east cheek wall of the north abutment
		West	LP-N-West	Lateral pressure cell installed on the west cheek wall of the north abutment
	South	Back	LP-S-Back	Lateral pressure cell installed on the backwall of the south abutment
		East	LP-S-East	Lateral pressure cell installed on the east cheek wall of the south abutment
		West	LP-S-West	Lateral pressure cell installed on the west cheek wall of the south abutment
In-place inclinometer	North	Back	IPI-N-Back	In-place inclinometer installed on the backwall of the north abutment
	South	Face	IPI-S-Face	In-place inclinometer installed on the face of the south abutment
		Back	IPI-S-Back	In-place inclinometer installed on the backwall of the south abutment

#### VERTICAL EARTH PRESSURES

The vertical pressures underneath the footing were measured with VPCs during the construction of superstructure elements (table 2), which included casting of the footing (pour 1), placement of the girders and deck panels, and casting of the concrete back and cheek walls above the footing (pour 2) until the bridge was opened to traffic. Long-term monitoring of the bridge continues to the present.

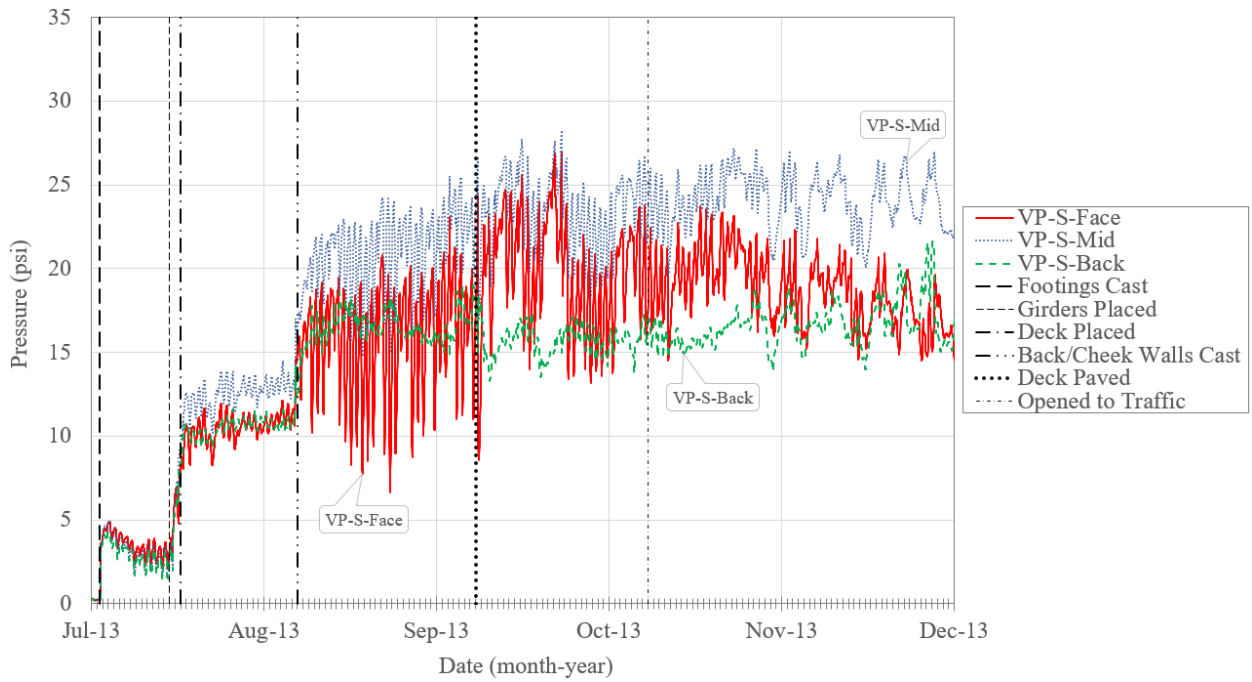
## **During Construction**

Figure 31 shows the measured vertical pressures during construction. The increase in pressure due to the deadweight of the bridge components can be clearly seen. Note that a software bug caused an error in the RDAS, so the pressure cell readings could not be read during construction for the north abutment (figure 31-A), but after the RDAS was reconfigured and the program was modified, the sensors were back online shortly after the deck was placed. The measured vertical pressures at the face and back of the footing are similar for both abutments, with the highest pressures measured in the middle of the footing on both abutments. For all VPCs, the daily fluctuation in measured vertical pressure dramatically increased after casting the back and cheek walls. These daily fluctuations represent the integration of the superstructure with the footings.



Source: FHWA.

A. Vertical earth pressures during construction of the north abutment.



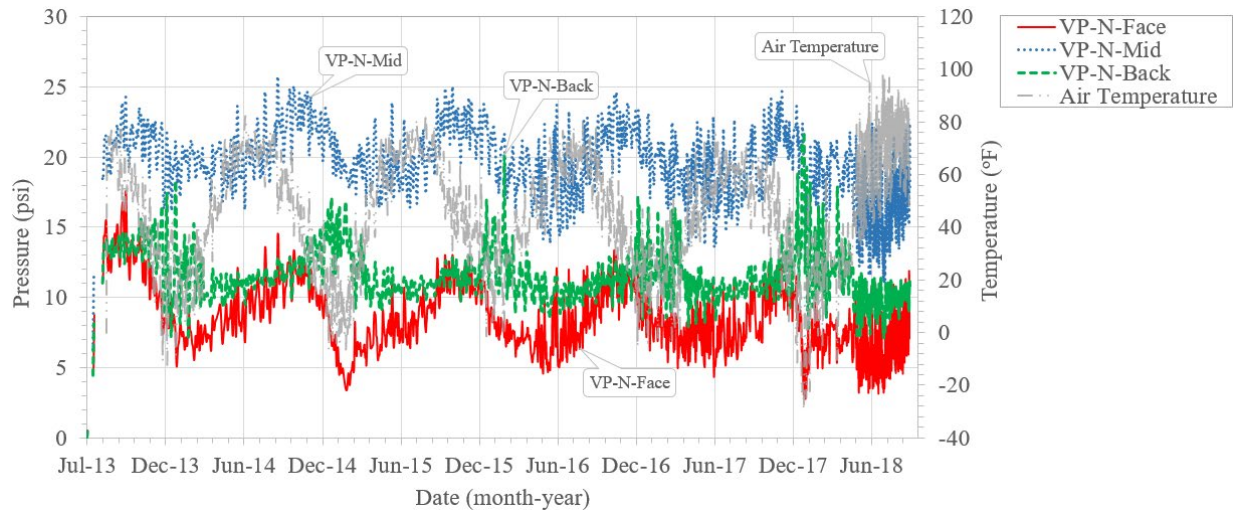
Source: FHWA.

B. Vertical earth pressures during construction of the south abutment.

**Figure 31. Charts. Vertical earth pressures during construction of the north and south abutments.**

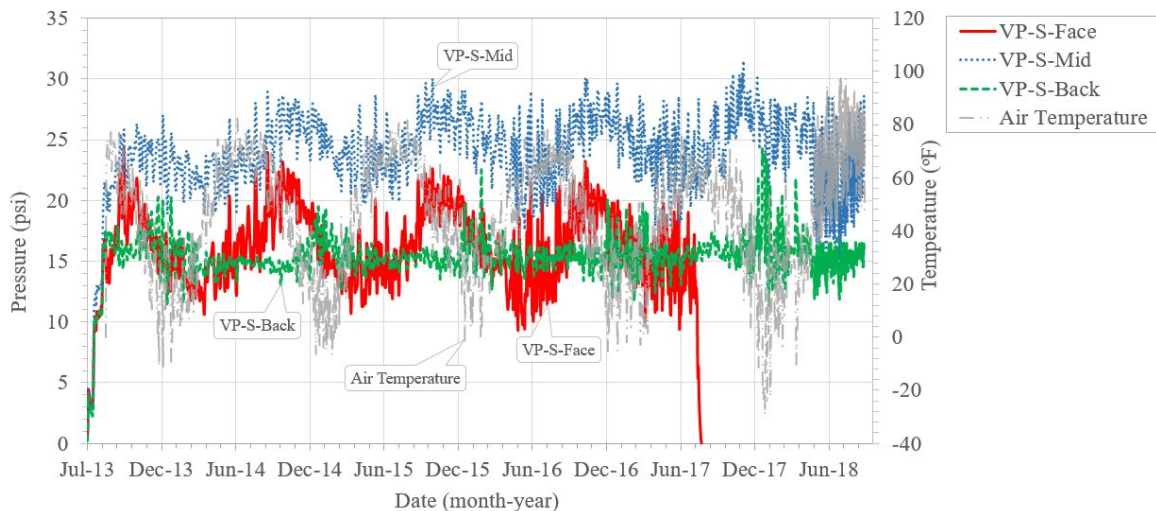
## Post-Construction

The measured vertical pressures for the north and south abutments throughout the 5-year monitoring period, July 2013 to August 2018, are shown in figure 32 along with the ambient air temperature (note the cell at the face of the south abutment malfunctioned in 2017). The plots show a seasonal fluctuation in vertical pressure due to the temperature (figure 32). As temperature increases and decreases, the superstructure expands and contracts, respectively, causing pressure fluctuations beneath the width of the concrete footing. The pressure signatures on each abutment are similar with slightly greater pressures on the south abutment. For both abutments, the highest pressures were recorded beneath the middle of the footing with face and back cell readings more equal.



Source: FHWA.

### A. Vertical earth pressures under north abutment footing.



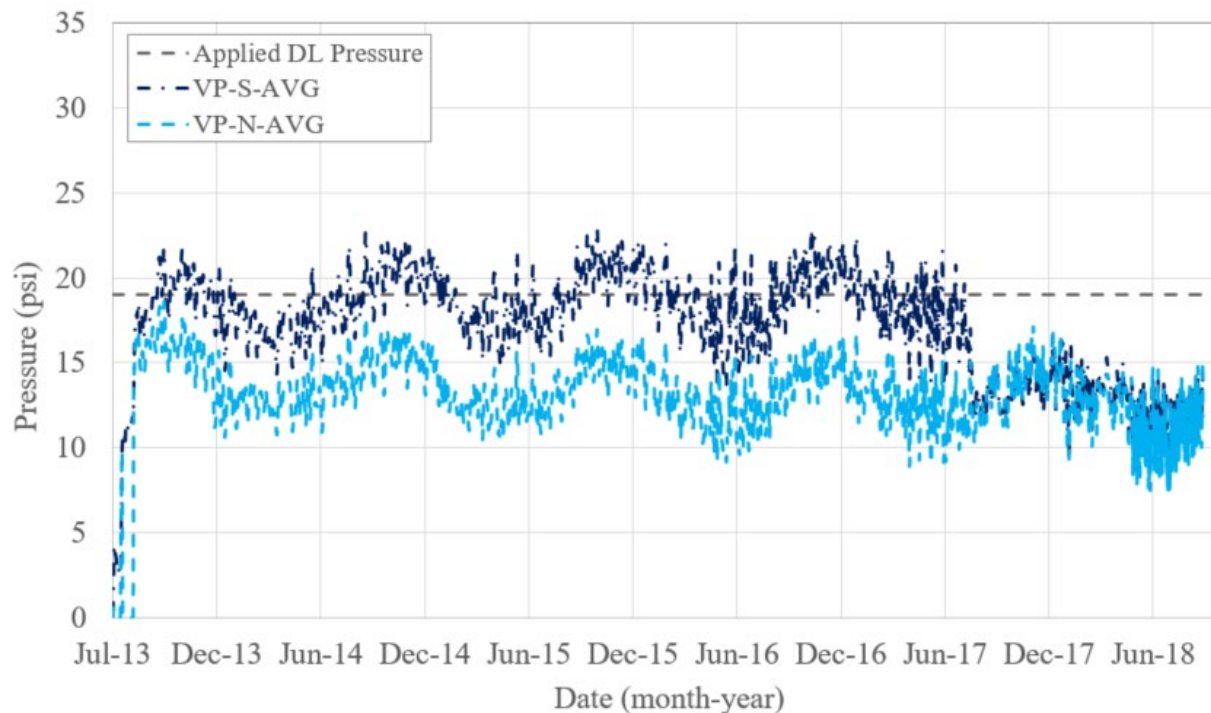
Source: FHWA.

### B. Vertical earth pressures under south abutment footing.

**Figure 32. Charts. Vertical earth pressures under north and south abutment footings.**

The VPC results for the face and middle portions of the footing show a general lag with seasonal temperature swings (figure 32). The vertical pressures at the back of the footing respond inversely to the air temperature; the maximum pressure occurs in sync with the dips in temperature. This correlation suggests a negative moment may occur as the superstructure contracts because the steel girders would cool down faster than the concrete bridge deck. The steel girders are less exposed to the sun, have a slightly lower thermal coefficient of expansion than concrete, and are cast into the concrete at the superstructure support ends. This restraint at the top (from the bridge deck) and back of the superstructure may, therefore, cause the increased pressures seen in the measurements toward the back of the footing. This restraint may also explain the lag in the pressures at the face and middle of the footing.

Figure 33 shows the average of the three VPCs beneath the footings of the north abutment (VP-N-AVG) and south abutment (VP-S-AVG). The average vertical pressures on the south abutment were about 5 psi higher than those on the north abutment. The south abutment reads closer to the engineer’s calculated DL pressure of about 19 psi (table 2). Note the average pressures for the south abutment after August 2017 are similar to those for the north abutment (once the cell at the face malfunctioned, it was not included in the dataset). Given that the backfill used is open-graded, there may be arching or inconsistent contact pressures across the VPCs (Nicks and Adams 2019), but the results provide a reasonably good estimate of the load.



Source: FHWA.

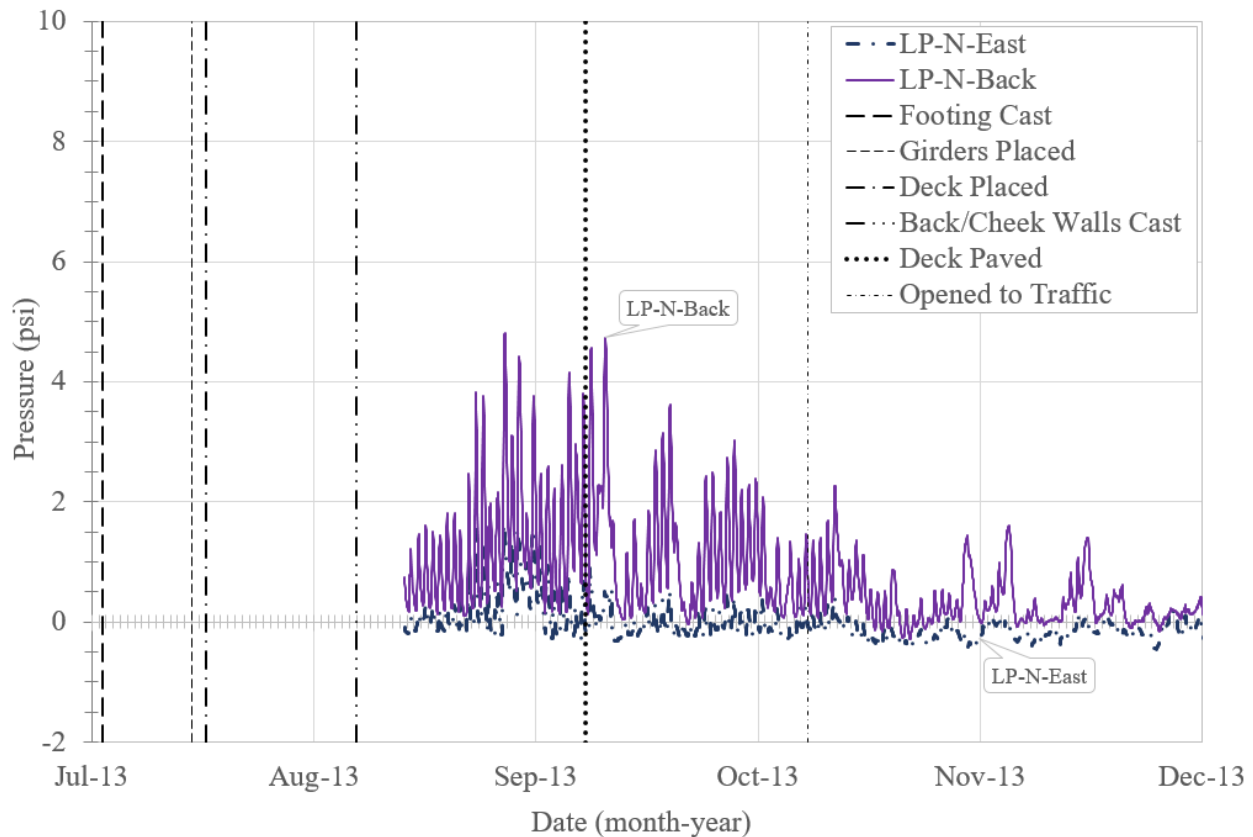
**Figure 33. Chart. Comparison of average vertical earth pressures on the north and south abutments.**

## LATERAL EARTH PRESSURES

CPCs were installed behind the backwall and along the cheek walls of the CR47 GRS-IBS to measure lateral earth pressures. The cells located on the backwall were installed to investigate thermal interaction between the integrated approach and superstructure; the cells located on the cheek walls were installed to evaluate any impacts due to the skew and superelevation of the superstructure.

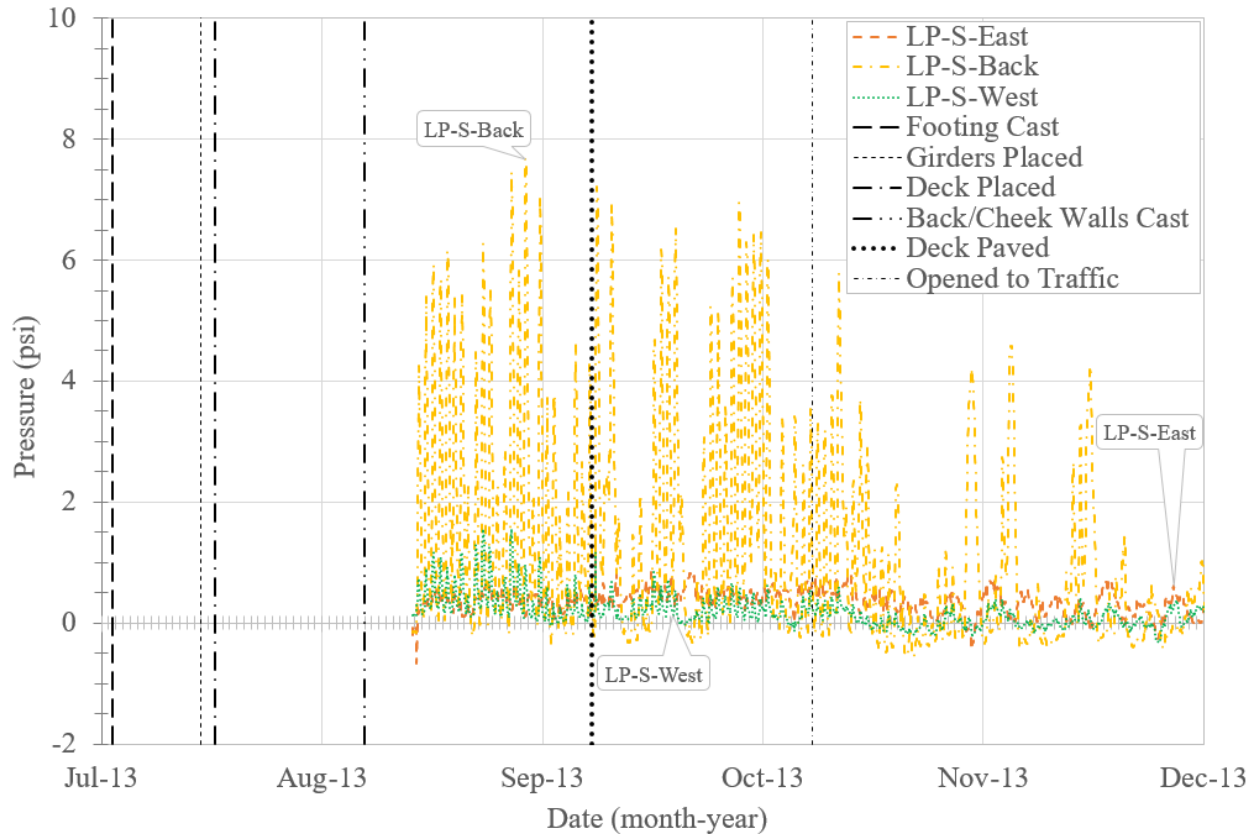
### During Construction

The CPCs were installed after the back and cheek walls were cast. Data collection began prior to construction of the integrated approach and pavement of the deck. The results show that initial backwall pressure readings spiked during the construction of both abutments and then leveled out more after the bridge was opened to traffic (figure 34); temperatures were also cooling off during that time of the year. Note the CPC installed on the west cheek wall of the north abutment malfunctioned at the beginning of data collection, so data are not available. Similar to the VPC readings, the CPC readings on the south abutment were higher than the north abutment, suggesting more thermal activity on the south bridge end, but the root cause is currently unknown.



Source: FHWA.

A. Lateral earth pressures on backwall and east cheek walls of the north abutment during construction.



Source: FHWA.

B. Lateral earth pressures on backwall and cheek walls of the south abutment during construction.

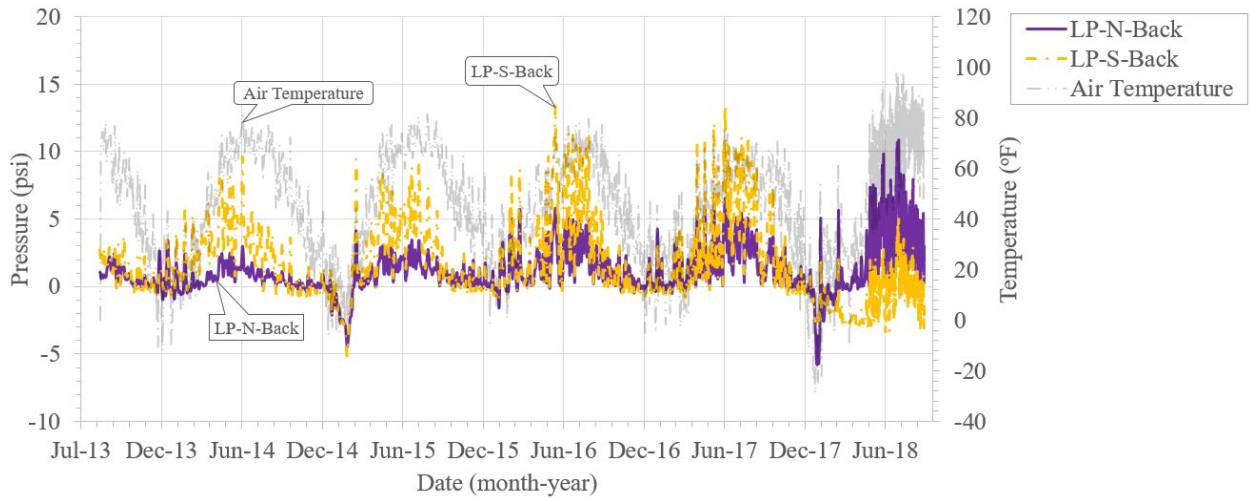
**Figure 34. Charts. Lateral earth pressures during construction of the north and south abutments.**

The pressure cells on the cheek walls measured significantly less lateral earth pressure values (<1 psi) than on the backwalls (figure 34). The results for the south abutment also indicate that there is not a big difference in lateral earth pressure activity between the east and west cheek walls; however, the pressures on the west cheek wall were slightly higher than those on the east cheek wall, particularly during construction activities. Regardless, the measured lateral cheek wall pressures correlate with at-rest ( $K_0$ ) conditions; using the assumed 40-degree friction angle and 110 lb/ft<sup>3</sup> unit weight, the theoretical at-rest earth pressure equals 0.82 psi.

### Post-Construction

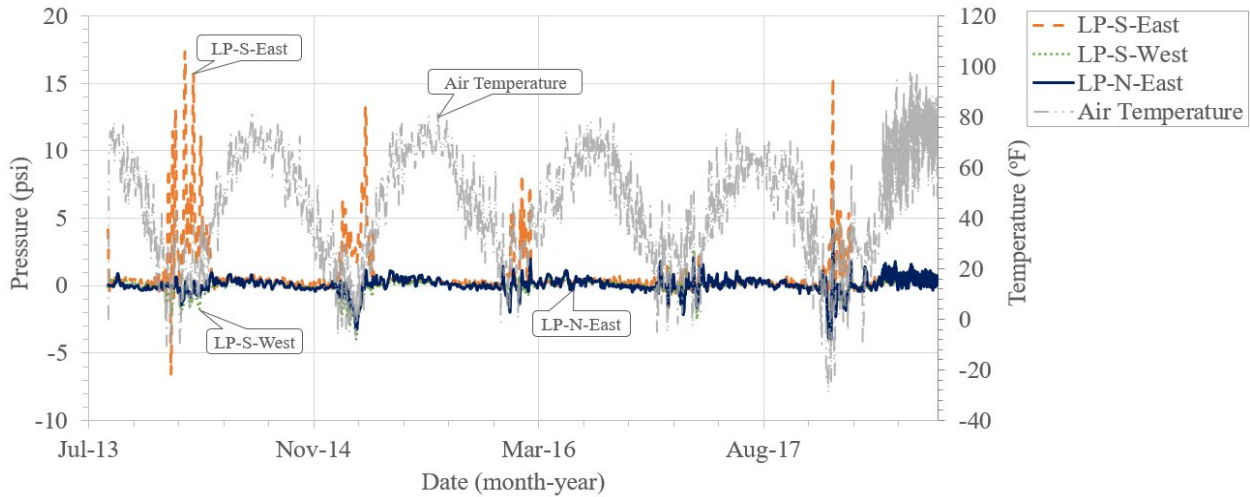
The measured lateral earth pressures on the back and cheek walls for the north and south abutments throughout the 5-year period of monitoring are shown in figure 35 and figure 36, respectively, along with the air temperature. The findings indicate a strong correlation between thermal movement of the superstructure and lateral earth pressures on the backwall. As the superstructure expands due to rising temperatures, it pushes the backwall against the integrated approach, increasing lateral earth pressures; vice versa, when the superstructure contracts due to cooling temperatures, the pressure against the backwall is relieved. The measured peak lateral

backwall pressures during the highest air temperatures are within the realm of the theoretical lateral stress under passive ( $K_p$ ) conditions; for full  $K_p$  conditions, the predicted lateral earth pressure is 10.5 psi.



Source: FHWA.

**Figure 35. Chart. Lateral earth pressures and temperatures behind backwalls.**



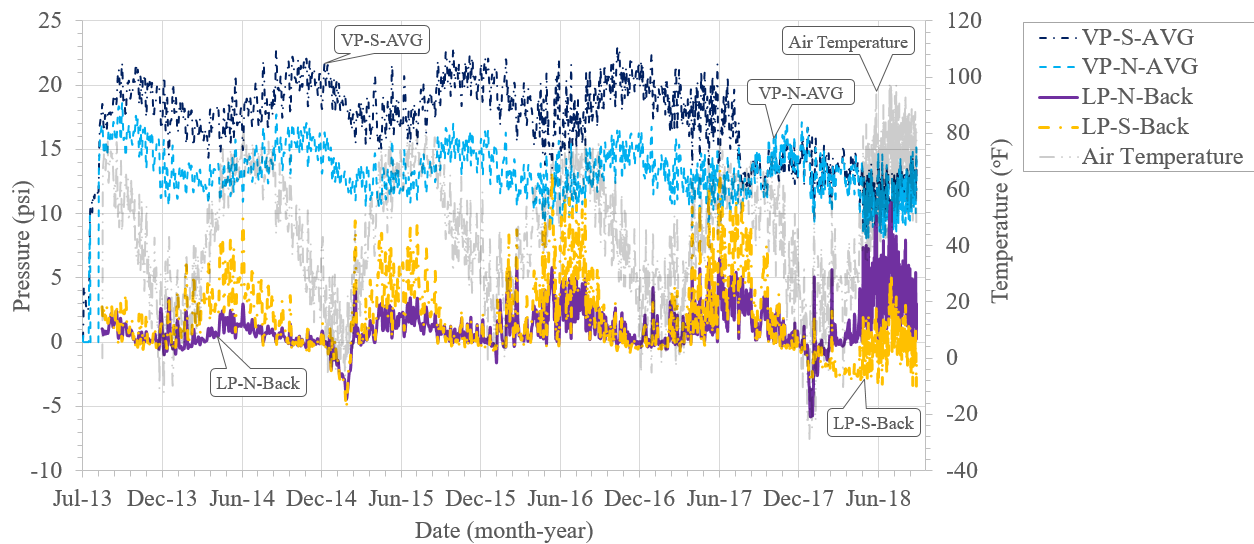
Source: FHWA.

**Figure 36. Chart. Lateral earth pressures on cheek walls.**

The lateral earth pressures on the north and south abutment backwalls are in alignment in terms of their cyclical nature; however, like the measurements taken during construction, the south abutment is experiencing more activity than the north. These results could be due to an instrumentation error, the placement of the CPCs, or the superstructure moving more in the south direction rather than the north (i.e., unequal expansion or contraction across the entire span length). The south abutment is slightly more elevated than the north, with the superstructure having a 0.5-percent grade.

Lateral earth pressures on the cheek walls are relatively inert compared to the backwall pressures, except for those on the east cheek wall of the south abutment, which exceed the backwall pressures (figure 36). The high pressure spikes against the east cheek wall of the south abutment only occur during the colder winter months. It is possible that water infiltrates the area around the pressure cell, and when the temperature dips below 32°F, the water freezes, expanding against the pressure cell, creating the pressure spikes.

The data suggest that the bridge tends to hump in cold temperatures causing increased vertical pressure toward the back of the footing, while the face and middle of the footing see a relative decrease in pressure. Comparing the change in vertical footing pressures and lateral backwall pressures, it appears that the superstructure might be transferring load to the backwall during the colder winter months; as the average vertical pressure decreases, the lateral pressures on the backwall increase (figure 37).

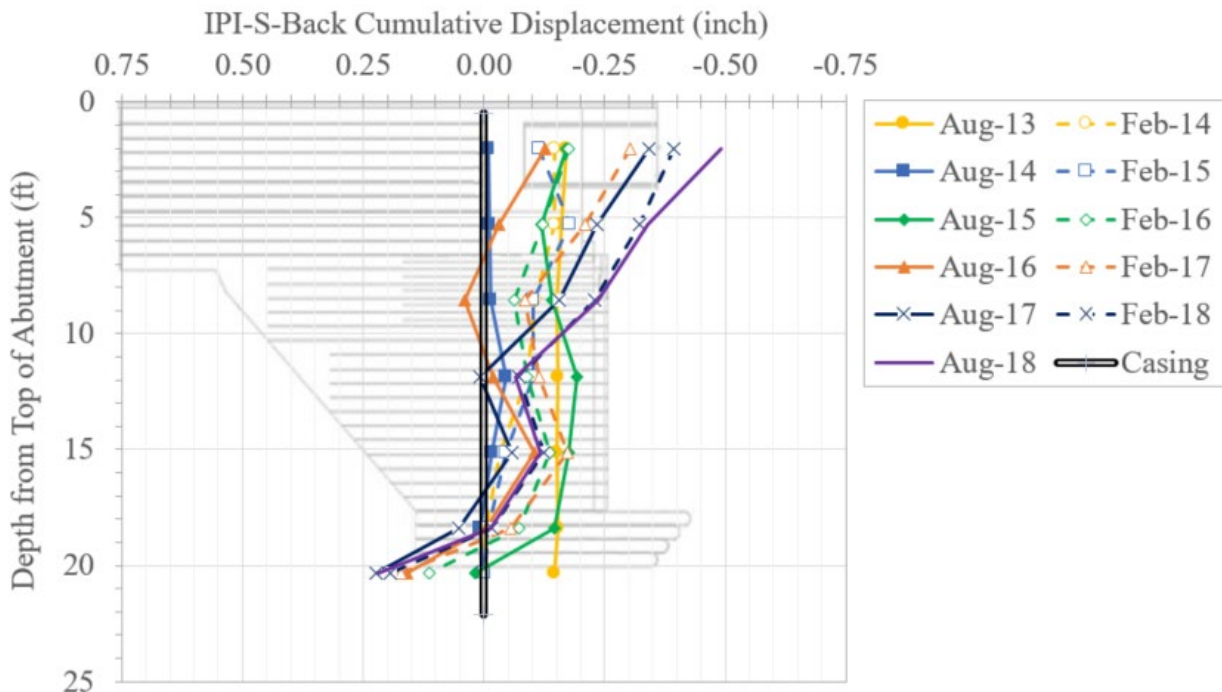


Source: FHWA.

**Figure 37. Chart. Relationship between vertical and lateral earth pressures for the north and south abutments.**

## Lateral Deformations

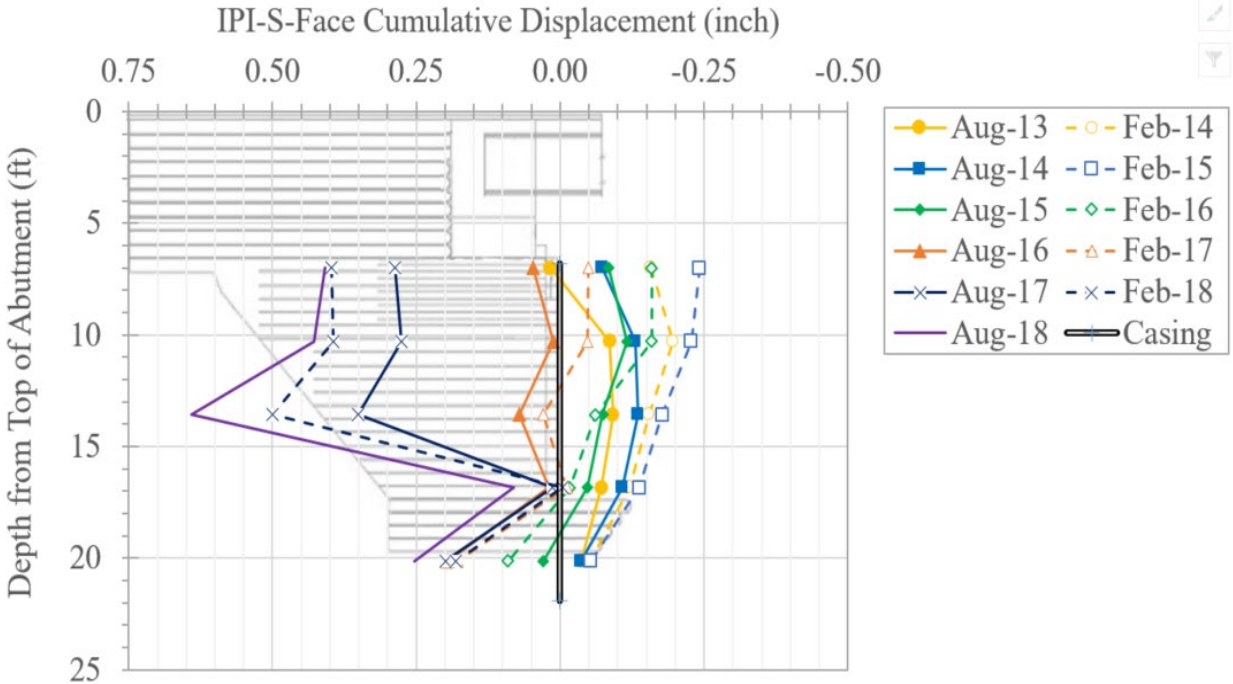
IPIs were installed directly behind the backwall of the superstructure on both abutments and on the south abutment wall to evaluate lateral deformations. In addition, comparing lateral deformations with earth pressures helped paint a bigger picture of the CR47 GRS-IBS's substructure–superstructure interactions during this 5-year period. A common way to display inclinometer measurements is through a cumulative displacement plot with depth. With cumulative displacement, the displacement at the top is assumed to equal the sum of the displacements measured from all sensors. Figure 38 through figure 40 show the resulting lateral deformation profiles based on cumulative displacement for IPI-S-Back, IPI-S-Face, and IPI-N-Back, respectively. Only data from August (summer) and February (winter) of each year are plotted to illustrate the movement of the abutment due to the thermal movement of the superstructure. The readings indicate a thermal response, moving outward in the positive direction (toward the abutment) and inward in the negative direction (toward the stream) as the superstructure expands and contracts, respectively.



Source: FHWA.

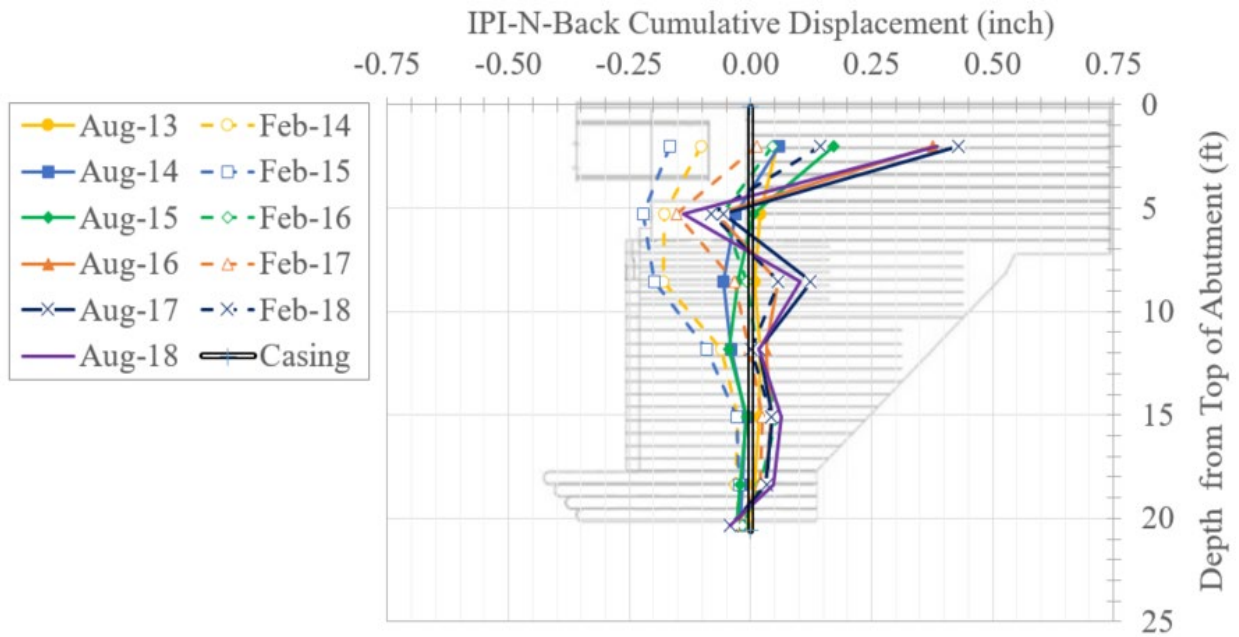
Note: GRS-IBS background is not to scale, and riprap is not shown.

**Figure 38. Chart. Cumulative displacement for IPI-S-Back.**



Source: FHWA.  
 Note: GRS-IBS background is not to scale, and riprap is not shown.

**Figure 39. Chart. Cumulative displacement for IPI-S-Face.**



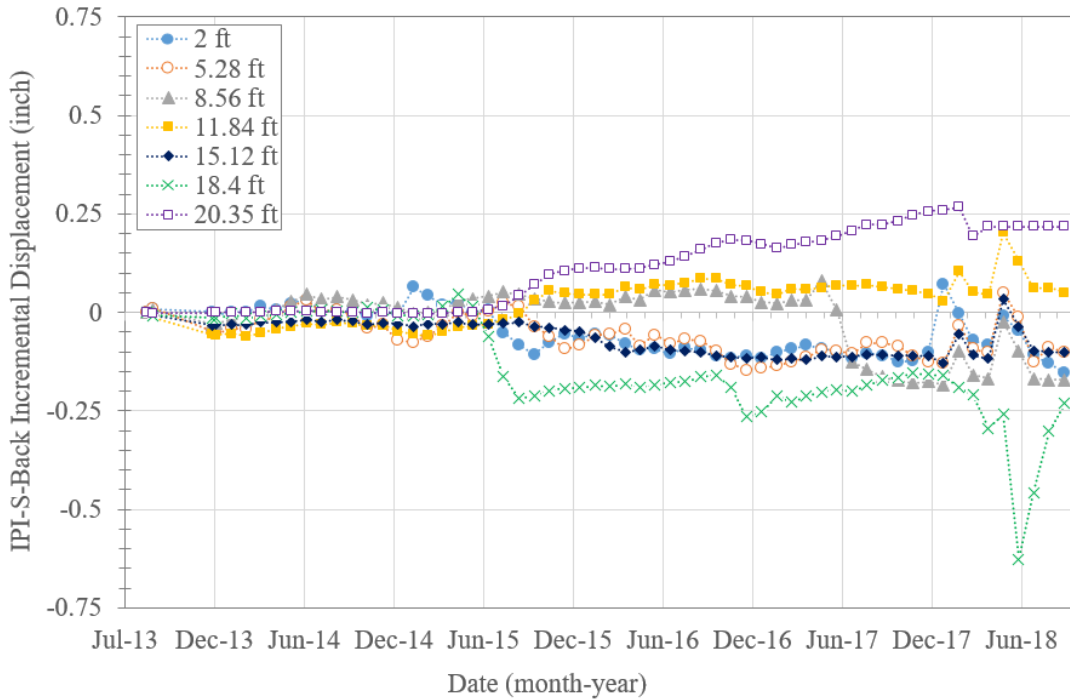
Source: FHWA.  
 Note: GRS-IBS background is not to scale, and riprap is not shown.

**Figure 40. Chart. Cumulative displacement for IPI-N-Back.**

The cumulative displacement profiles for the IPIs installed behind the backwall and at the face of the south abutment are questionable (figure 38 and figure 39); it is suspected that errors were produced by the south abutment IPI sensors. For example, the bottom IPI sensors show movement even though they were installed in the dense till foundation. Additionally, the pattern of the movement of the IPI sensors do not show the thermal movement of the abutment due to expansion and contraction of the superstructure, only contraction, which is questionable. Such results likely indicate random sensor drift with compounded error added upward toward the top of the abutment.

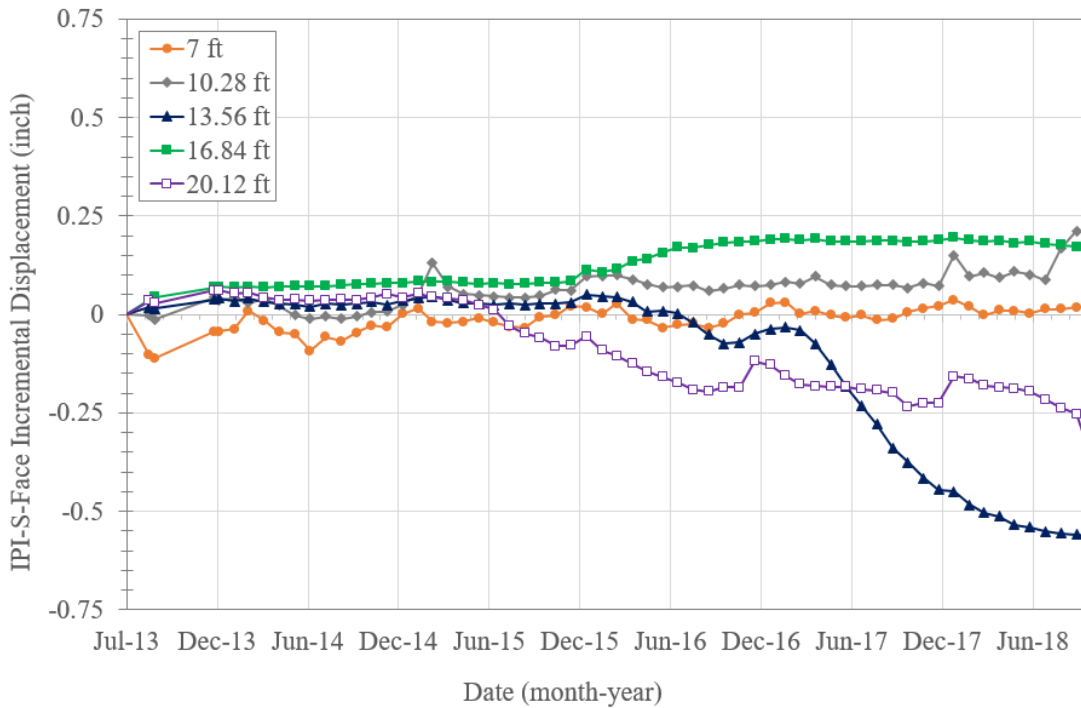
The IPI on the north abutment remained stable, showing movement at the top third of the abutment (figure 40). An inflection point is seen near the base of the footing due to the initial movement of the abutment in the negative direction occurring during contraction of the superstructure. Additionally, the plot indicates that the abutment moves with the superstructure during the seasonal thermal cycles; the cumulative seasonal movement is between approximately 0.13 and 0.35 inch, depending on the year.

With cumulative displacement profiles, if any sensor is off, the systematic error compounds as displacement is calculated up the height of the inclinometer. As an alternative to this approach, incremental displacement was evaluated over time for each individual sensor in IPI-S-Back, IPI-S-Face, and IPI-N-Back (figure 41, figure 42, and figure 43, respectively). The data show the movement of the sensors at each depth is relatively similar until about 2015, when more apparent deviations began to occur due to sensor instability (drift). The largest and most active incremental movements occurred 2 ft from the top of the roadway for IPI-N-Back (figure 43), with an approximate movement of 0.5 inch between December 2017 and June 2018. While seasonal cyclic movement is observed at the top of the north abutment backwall, with movement toward the bridge during winter months (contraction) and vice versa during summer months (expansion), the trend seems to show the IPI progressively moves in the positive direction toward the abutment/approach (i.e., away from the stream). However, the IPI sensor at 5.28 ft below the top sensor shows a slight negative movement toward the stream, suggesting the bridge footing might have rotated slightly.



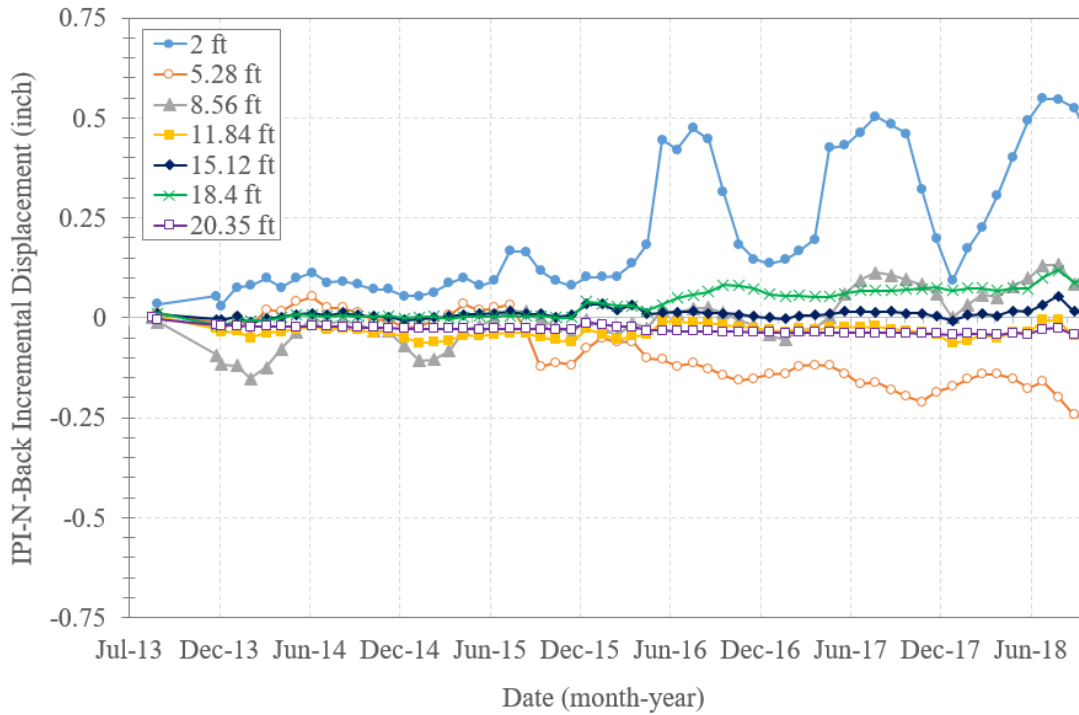
Source: FHWA.

**Figure 41. Chart. Incremental displacement for IPI-S-Back.**



Source: FHWA.

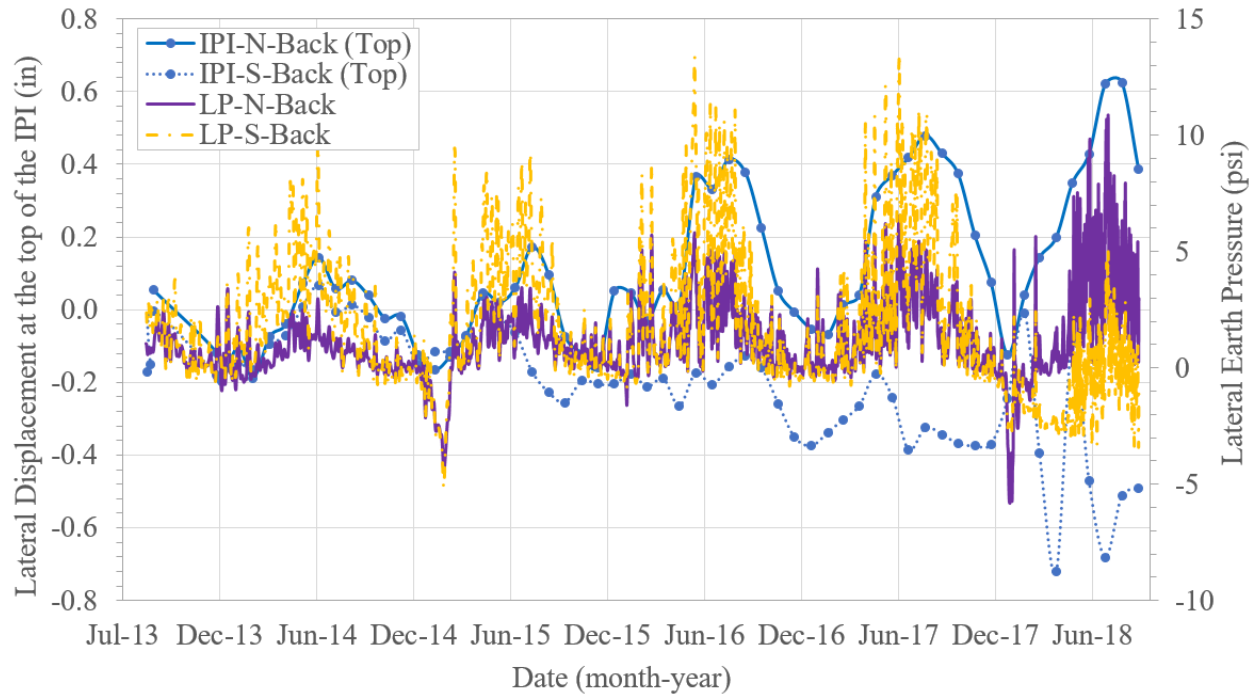
**Figure 42. Chart. Incremental displacement for IPI-S-Face.**



Source: FHWA.

**Figure 43. Chart. Incremental displacement for IPI-N-Back.**

The displacement of the backwall due to thermal superstructure movements should have an impact on the measured lateral earth pressures from the CPCs. For the CR47 GRS-IBS, this relationship was clear for the north abutment; data show a positive relationship between the cumulative displacement at the top IPI backwall sensor and the lateral earth pressure behind the backwall (figure 44). As air temperature increases, the superstructure expands, pushing the backwall toward the integrated approach (positive direction) causing an increase in lateral earth pressures. Likewise, as the superstructure contracts (negative direction), the backwall lateral earth pressures are relieved. This trend is only seen at the beginning for the south abutment, deviating in 2015, perhaps due to sensor drift or other errors within the instrumentation.

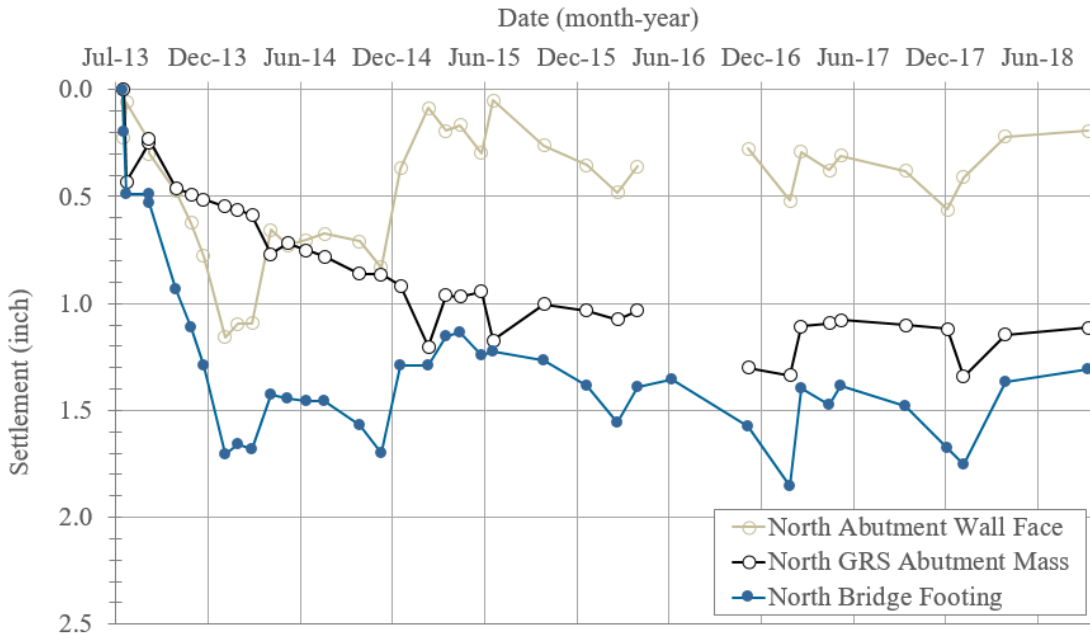


Source: FHWA.

**Figure 44. Chart. Relationship between maximum cumulative IPI displacement and lateral earth pressures behind the backwalls.**

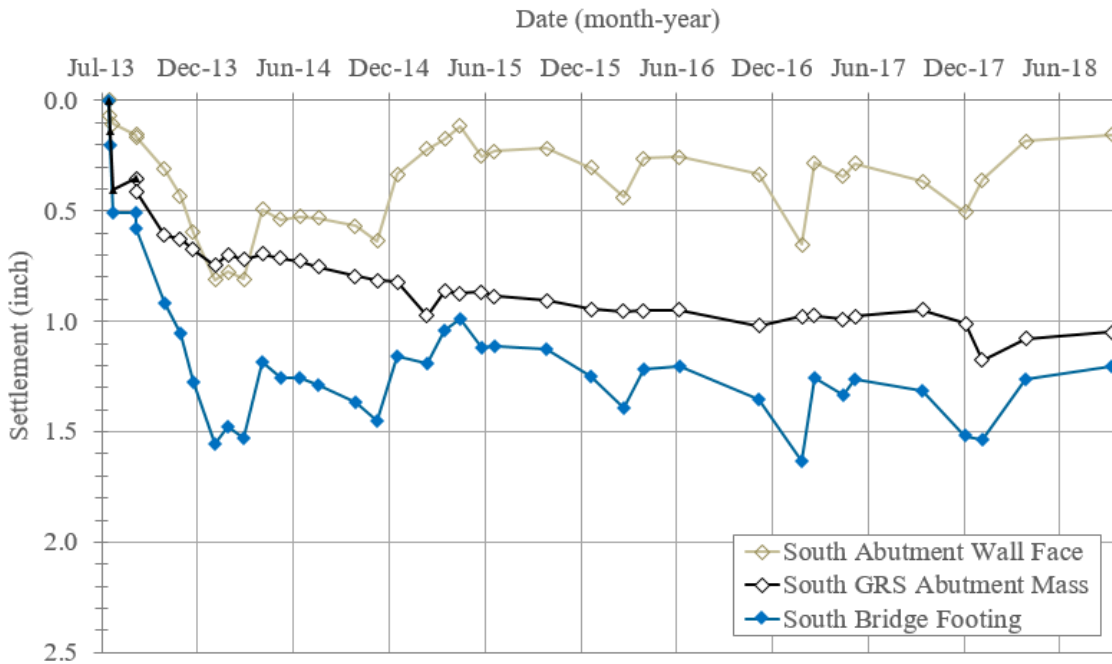
### Vertical Settlement and Strain

Survey targets were installed on the wall face and on the footings of both abutments to measure total settlement and compression of the reinforced backfill within the GRS abutment. Since the modular block wall facing is relatively incompressible, the settlement it experiences is isolated to the native foundation soils beneath the abutment and RSF. The footing, on the other hand, experiences the total settlement, a combination of both the settlement of the native foundation soils and compression of the reinforced backfill within the GRS abutment. By finding the difference between the footing and wall measurements, the compression of the GRS abutment can be isolated from that of the foundation settlement. Figure 45 shows the bridge footing (total settlement), wall face (foundation settlement), and computed settlement of the GRS-abutment mass for the north and south abutments. The 5-year settlement record shows some seasonal fluctuations, which are perhaps due to the swelling or freezing of foundation soils. Figure 46 illustrates the compression of the GRS abutment mass due to the deadweight of the superstructure in terms of strain (as a function of the wall heights of the north and south GRS abutments, which are of 11.0 and 11.6 ft, respectively).



Source: FHWA.

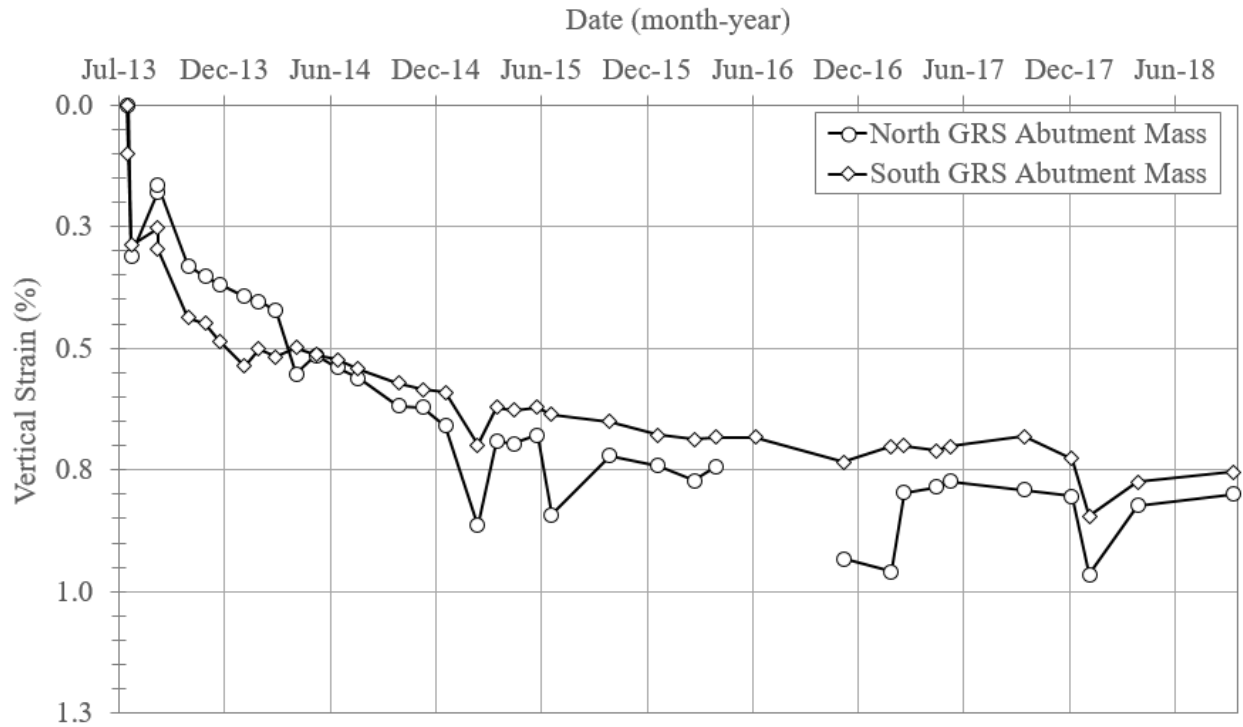
A. North abutment settlement.



Source: FHWA.

B. South abutment settlement.

**Figure 45. Charts. Vertical settlement of the north and south abutments.**

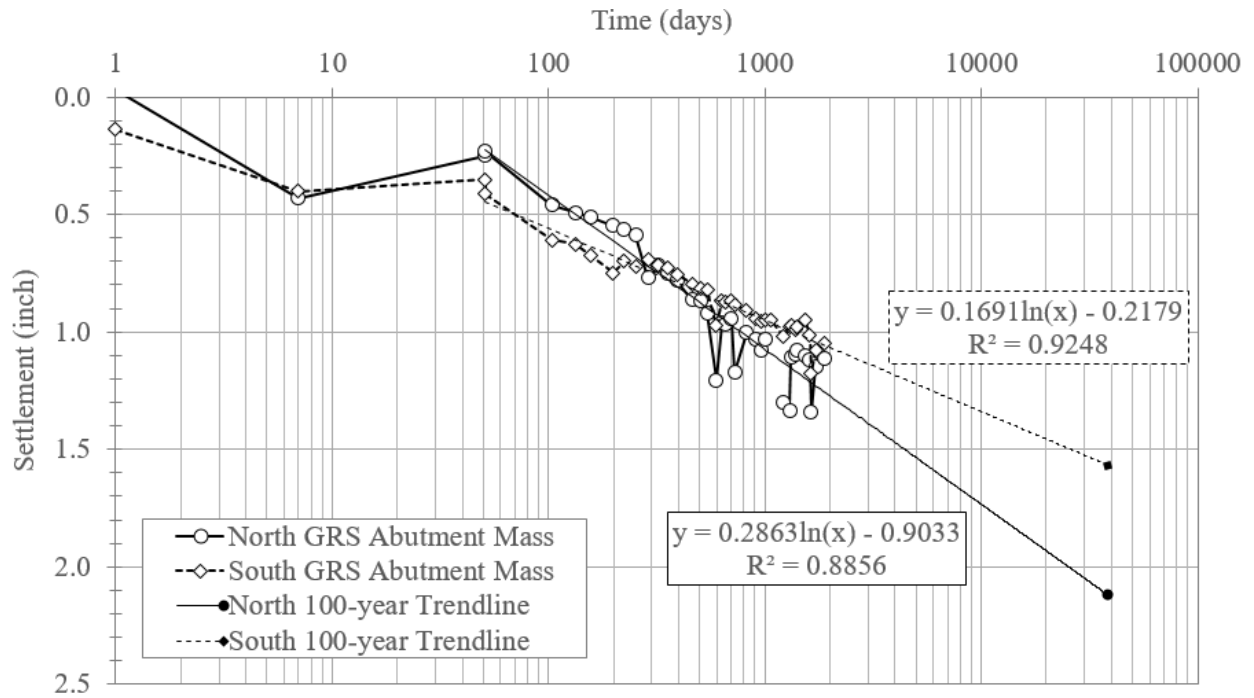


Source: FHWA.

**Figure 46. Chart. Vertical strain of the abutments based on their height.**

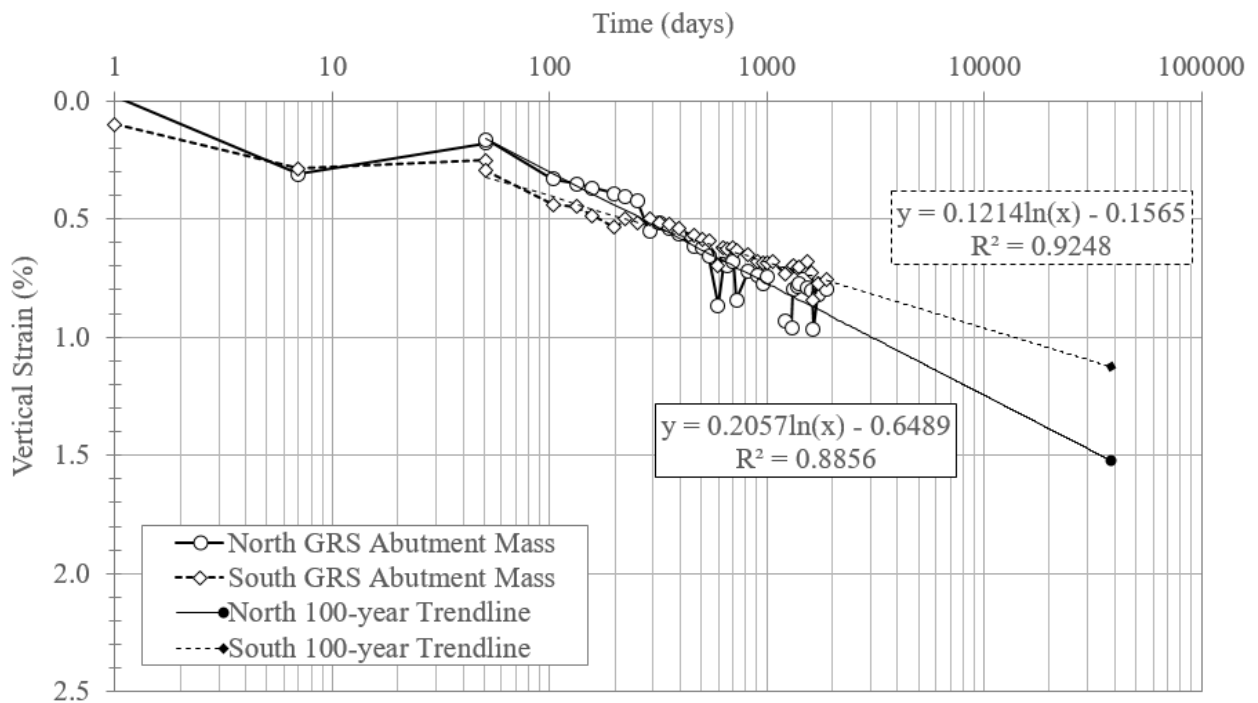
The total footing settlement is about 1.3 and 1.2 inches for the north and south abutments, respectively. Compression of the north and south GRS abutment masses is about 1.1 and 1.05 inches, respectively; based on the abutment heights, these measured settlements equate to 0.8 and 0.75 percent vertical strain after 5 years. The immediate strain was about 0.34 percent, less than the typical tolerable vertical strain of 0.5 percent. Secondary compression of the GRS backfill should also be considered in GRS design to ensure the clear space is adequate. To forecast the long-term settlement after 100 years (typical bridge design life), settlement and strain can be graphed in a semi-log plot (figure 47). A lognormal relationship is found between the settlement/strain and the number of days. After 100 years (36,500 days), that relationship suggests that the north and south abutments will settle (and strain vertically) 2.1 inches (1.5 percent) and 1.6 inches (1.1 percent), respectively. These values are below the minimum clear space recommendation of 3 inches or 2 percent of the wall height (Adams and Nicks 2018).

There is some differential settlement between the north and south abutments, but the magnitude is small and well below tolerable angular distortion for the superstructure. The differential settlement for the GRS abutment masses and the footings between the north and south abutments is shown in figure 48. After 5 years, the angular distortion (i.e., the ratio of the differential settlement to the span length [105 ft]) is about 0.0003. This angular distortion value is one order of magnitude below the American Association of State Highway and Transportation Officials angular distortion criteria limits of 0.008 for simple span bridges (AASHTO 2017). For the projected 100-year settlements (figure 47-A), the forecasted maximum angular distortion is 0.0004.



Source: FHWA.

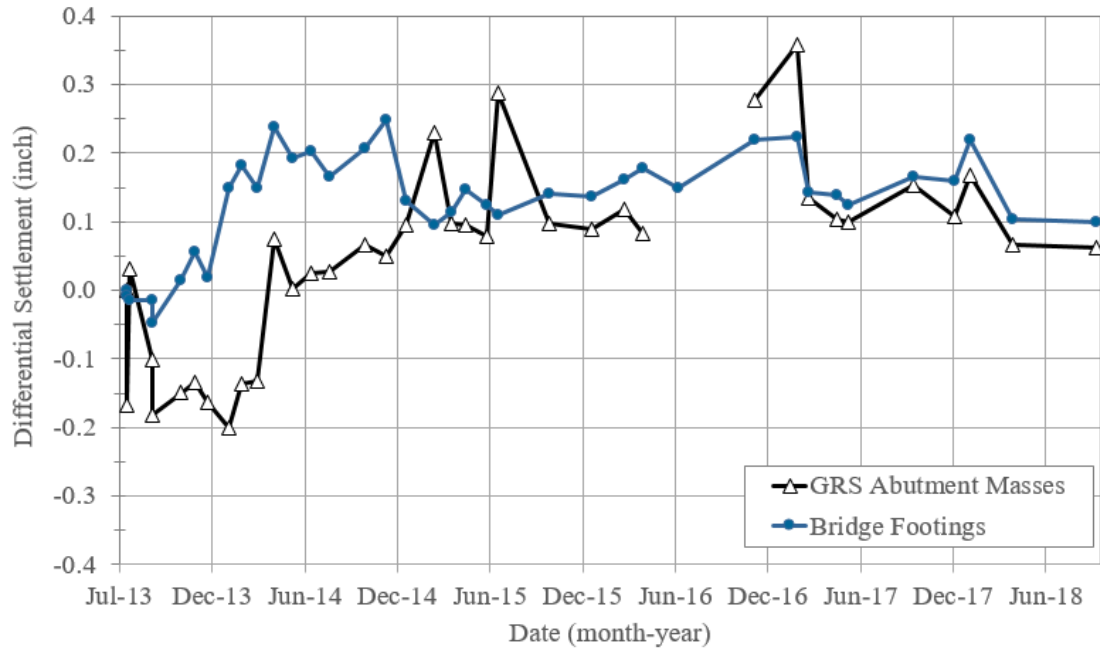
A. 100-year settlement forecast.



Source: FHWA.

B. 100-year vertical strain forecast.

**Figure 47. Charts. 100-year forecast for settlement and vertical strain of the north and south abutments.**



Source: FHWA.

**Figure 48. Chart. Differential settlement between the north and south abutments.**



## CHAPTER 4. SUMMARY AND CONCLUSIONS

This project incorporated a suite of instrumentation to evaluate the performance of the CR47 GRS-IBS in St. Lawrence County, NY. After 5 years of monitoring efforts, the results indicate that the GRS-IBS is performing as well as expected. The seasonal temperature changes create interesting substructure–superstructure interactions between the bridge and the GRS abutments. Vertical and lateral earth pressures along with lateral deformations are all impacted by seasonal variations in temperature. The vertical settlement may also be affected, but the frequency of data collection does not allow for that trend to be established (or negated). The GRS-IBS responds actively, but predictably, to the external loads from the structure. The measured deformations after 5 years are negligible in terms of adversely impacting performance. In summary, the following results were found throughout this data analysis:

- The VPCs captured the incrementally applied DL during construction. After the bridge was opened to traffic, the applied vertical pressure leveled off, only oscillating with temperature (figure 31).
- The VPC installed in the middle of the footing width read the highest readings, with the VPCs in the front and back measuring relatively similar vertical earth pressures to each other. There was a lag between the VPC readings and air temperature for the front and middle VPCs. The VPC at the back of the footing was in phase with the temperature during colder months, increasing with decreasing temperature. One explanation for this difference is that the concrete deck, backwalls, and check walls constrained thermal contraction of the steel girders, causing the girders to hump slightly and transfer load to the back of the semi-integral abutment footing (figure 32).
- The measured lateral earth pressures against the check walls are significantly smaller and less active than those against the backwalls for both abutments (figure 35 and figure 36).
- The lateral earth pressures increase as the superstructure expands and decrease as the superstructure contracts. During expansion, the average vertical load from the footing is transferred to the backwall (figure 37).
- The IPI readings on the abutments indicate a thermal response, moving out (toward the abutment) and in (toward the stream) as the superstructure expands and contracts, respectively (figure 38 through figure 40). It is suspected that the sensors malfunctioned between 2015 and 2016 based on incremental displacement readings for the south abutment.
- There was a clear relationship between the displacement of the backwall during thermal movements and the measured lateral earth pressures behind the backwall for the north abutment (figure 44); suspicious data on the south abutment precluded this comparison.

- The total settlement of the footings is about 1.3 and 1.2 inches for the north and south abutments, respectively (figure 45 and figure 46). Based on the abutment heights, these results equate to 0.8- and 0.75-percent vertical strain, respectively, after 5 years (figure 47).
- Differential settlement for the superstructure is very small, with the maximum measured angular distortion over the five-year time span an order of magnitude below the tolerable limit for bridges.
- To forecast the settlement after 100 years (design life of the bridge), settlement (and strain) was graphed in a semi-log plot (figure 47). After 100 years (36,500 days), the north and south abutments are predicted to settle (and strain vertically) 2.1 inches (1.5 percent) and 1.6 inches (1.1 percent), respectively. These movements are tolerable but suggest secondary compression of the granular backfill within the GRS abutment cannot be ignored in design.

## REFERENCES

- AASHTO. 2017. *M 145: Standard Specification for Classification of Soils and Soil–Aggregate Mixtures for Highway Construction Purposes*. Washington, DC: AASHTO.
- Adams, M. T. and J. E. Nicks. 2018. *Design and Construction Guidelines for Geosynthetic Reinforced Soil Abutments and Integrated Bridge Systems*, FHWA Report No. HRT-11-026. Washington, DC: Federal Highway Administration.
- Adams, M. T., J. E. Nicks, T. Stabile, J. T. H. Wu, W. Schlatter, and J. Hartmann. 2011. *Geosynthetic Reinforced Soil Integrated Bridge System Interim Implementation Guide*, FHWA Report No. FHWA-HRT-11-026. Washington, DC: Federal Highway Administration.
- ASTM D2487. 2017. *Standard Practice for Classification of Soils for Engineering Purposes (Unified Soil Classification System)*. West Conshohocken, PA: ASTM International. DOI: <https://doi.org/10.1520/D2487-17>.
- Nicks, J. E. and M. T. Adams. 2019. “Lateral Earth Pressure Distribution with Depth for GRS Mini-Abutments.” In *Proc. of Geosynthetics 2019*. Houston, TX: Industrial Fabrics Association International.
- State of New York Dept. of Transportation. 2014. *Standard Specification (US Customary Units)*. Albany, NY: New York State Dept. of Transportation. Accessed July 2, 2019. [https://www.dot.ny.gov/main/business-center/engineering/specifications/english-spec-repository/espec1-9-14english\\_0.pdf](https://www.dot.ny.gov/main/business-center/engineering/specifications/english-spec-repository/espec1-9-14english_0.pdf).





